SAND2021-12973R

Molten Salt Reactor Passive Heat Removal System Modeling

Dallin J Keesling

September 2021

U.S. DEPARTMENT OF ENERGY

National Nuclear Security Administration

Sandia National Laboratories is a multimission laboratory managed and operated by National Technology and Engineering Solutions of Sandia, LLC, a wholly owned subsidiary of Honeywell International Inc., for the U.S. Department of Energy's National Nuclear Security Administration under contract DE-NA0003525.

SAND2021-12973 R

CONTENTS

LIST OF FIGURES

LIST OF TABLES

ACRONYMS AND DEFINITIONS

Abbreviation	Definition
CFD	Computational Fluid Dynamics
DHX	DRACS Heat Exchanger
DRACS	Direct Reactor Auxiliary Cooling System
MSR	Molten Salt Reactor
PB-FHR	Pebble-Bed Fluoride-Salt-Cooled-High-Temperature-Reactor
TCHX	Thermosyphon-Cooled Heat Exchanger
TRISO	Tri-structural-ISOtropic

1. INTRODUCTION

Molten salt reactors (MSRs) are a group of advanced nuclear reactor designs proposed for possible implementation as part of the generation IV nuclear reactor fleet. Their use of molten salt coolants allow them to operate safely at much higher temperatures than conventional water-cooled nuclear reactors, and can be operated near to atmospheric pressure. Some MSR designs directly mix fissile material with the coolant allowing fissile material and fission products to flow freely through the reactor, allowing for online refueling. Some implement conventional nuclear fuel, and simply rely on molten salt as a coolant. Others, such as the Berkeley Mark I Pebble-Bed Fluoride-Salt-Cooled High Temperature Reactor (PB-FHR) encapsulate fuel in TRISO pebbles which can be circulated through a molten salt coolant, allowing for online refueling and fission product removal without mixing the coolant and fuel together.

As with conventional light-water reactor designs, all MSRs require a method to safely and reliably remove decay heat from the reactor core if primary cooling systems are unavailable. Ideally, these heat removal systems will operate passively, so that the fuel can be adequately cooled without access to electric power or operator interference. One such passive heat removal system employed in the Mark I PB-FHR design is the Direct Reactor Auxiliary Cooling System.

1.1. Direct Reactor Auxiliary Cooling System

The DRACS operates by natural convection to transfer heat from the reactor vessel to a secondary salt loop through the DRACS Heat Exchanger (DHX). The secondary salt loop similarly flows by natural convection from the DHX to a second heat exchanger, the Thermosiphon-Cooled Heat Exchanger (TCHX) where it is cooled by radiative heat transfer to tube banks of water. The water, now turned to steam, is subsequently cooled by passing through an air-cooled condenser after which it returns to the water supply tank. With zero dependence on external action, a DRACS loop is designed to remove 1% of the nominal reactor power (2.36 MW) indefinitely. Each PB-FHR is equipped with three DRACS loops, which is sufficient to match the rate of decay heat production in the core within approximately two minutes of reactor scram. A full description of the Mark I PB-FHR and its DRACS system is available in the public domain [1].

1.2. Salt Properties

$LiF\text{-}BeF_2$, more commonly referred to as FLiBe, is the chosen molten salt coolant for many MSR designs. At operating temperatures, it has a viscosity and heat capacity comparable to water, which makes it very attractive as a circulating coolant. Additionally, FLiBe has a very high boiling point at atmospheric pressure, over $1430°C$, so it is an ideal candidate for low-pressure operations. Detailed study of molten salt properties is an ongoing endeavor, but average thermophysical properties at operable temperatures are sufficiently well characterized for processes that experience small temperature changes. The values chosen for salt properties in this work are presented in Table A-2.

2. METHODS

2.1. OpenFOAM Model

2.1.1. Assumptions

A few key assumptions were applied when developing the model, most of which relate to the fluid properties chosen. Due to the developing nature of FLiBe salt properties, different models have been proposed to relate various thermophysical properties with temperature. For this model, correlations were chosen from the Engineering Database of Liquid Salt Thermophysical and Thermochemical Properties developed by Idaho National Labs [2]. To limit model development time and computational cost, these correlations were used to calculate an average value to represent salt performance across the expected temperature range. This approach was used to provide a constant value for fluid viscosity, heat capacity, thermal conductivity, and Prandtl number.

All surfaces are assumed to be smooth, adiabatic surfaces, and thermal expansion of the piping is neglected.

2.1.2. Geometry

The DRACS systems consists of two heat exchangers, the DHX and TCHX, connected by stainless steel pipe. The original design documentation [1] does not specify the size of these connecting pipes, but after inspection of 3D CAD models provided in the documentation, 6-inch pipe schedule 80 stainless steel pipe was chosen for this model. Similarly, the pipe lengths were not specified in the original document but were determined based on inspection of the CAD model and the provided salt volume.

Since the purpose of this model is to evaluate how degraded DRACS performance affects the reactor vessel temperature during an accident scenario, the heat exchangers proposed for the original design are not modeled fully in this OpenFOAM model. Instead, representative heat exchangers are modeled that share the same total volume as the heat exchangers presented in the design documentation. Details of how these heat exchangers were modeled is presented in 2.1.5 Heat Exchanger Model Functionality.

The overall geometry used for the calculations is shown in Figure 2-1.

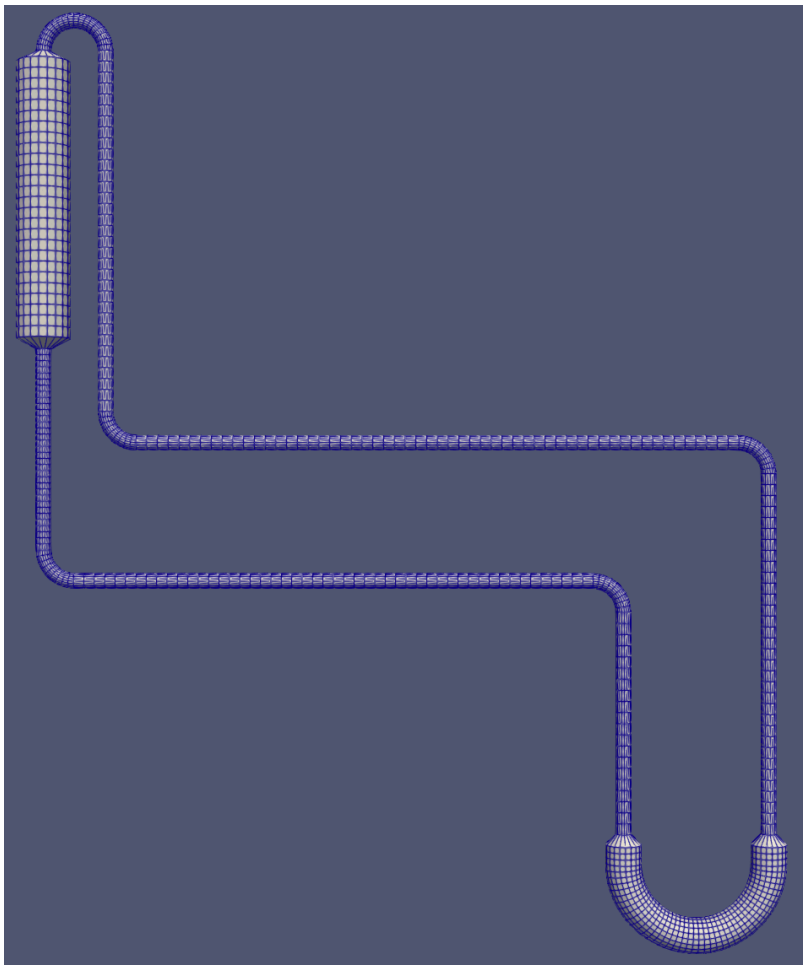

Figure 2-1 DRACS Loop Geometry. TCHX on the upper left, DHX on bottom right.

Two different mesh strategies were used for this model. First, the geometry was finely meshed all the way up to the pipe walls to resolve the viscous sublayer. The mesh for this first case is shown in Figure 2-2. This mesh used a total of 1,444,000 cells. Good practice in transient CFD modelling is to limit the Courant number to some value below 1 in all cells. To achieve this, a very small timestep was required. Early testing projected that this model would take approximately a month to calculate a single hour using available tools. Since the scenarios to be modeled were several hours long, this mesh was deemed infeasible with such small timesteps. However, this mesh was useful in determining what steady state conditions should be expected, which aided in validating the second meshing strategy employed in this work.

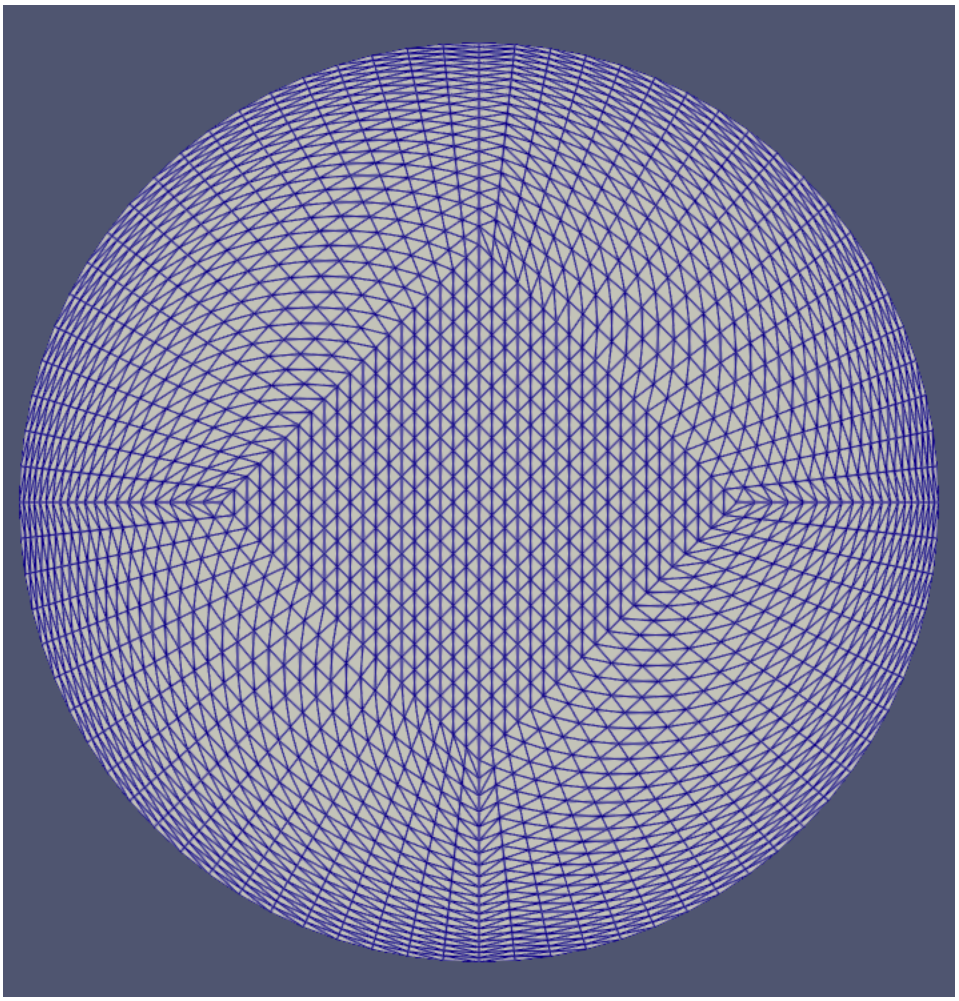

Figure 2-2. The first version of the model mesh. Cells are most refined near the pipe walls. 1,444,000 cells in total.

After it was determined that the first mesh design was computational prohibitive, a second mesh was chosen that depends on wall functions to estimate the effects of the viscous sublayer. This second mesh, as shown in Figure 2-3, does not finely resolve the viscous sublayer and uses far less cells overall. In fact, the use of wall functions requires that the cells near the wall be sufficiently large to be outside the viscous sublayer entirely. While the cross-sectional mesh density was decreased considerably, the mesh density in the flow direction was maintained. In terms of performance, the final mesh design allows the model to calculate an hour of simulation time in approximately 5 hours, making this design feasible for the degradation study.

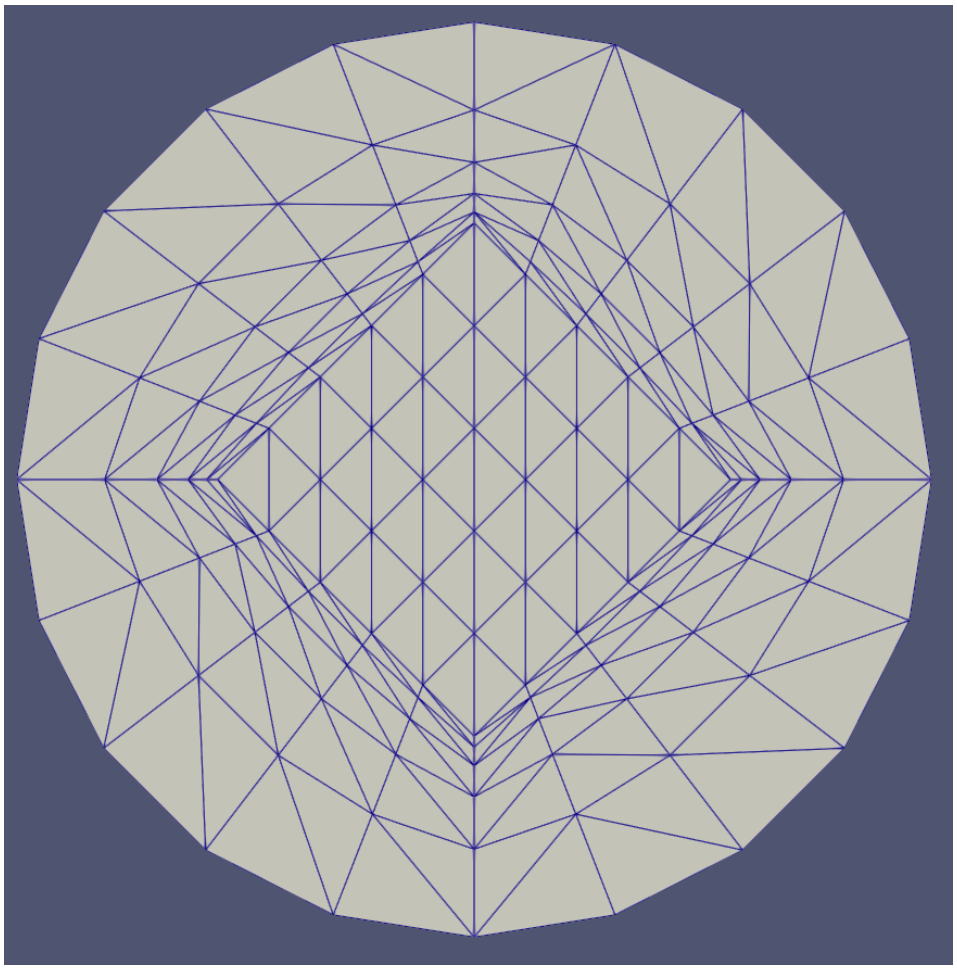

Figure 2-3. Final Mesh design. Increases the cell size near the pipe walls to take advantage of wall functions to estimate effects of the viscous sublayer. 44625 cells in total.

2.1.3. Turbulence Modeling

Based on flow information available in the DRACS technical description [2], the Reynolds number for flow through the DRACS loop is approximately 17500, which places it firmly in the turbulent flow regime. A Reynolds-Averaged Solver (RAS) was used to model the effects of turbulence in the OpenFOAM model, utilizing the k-ω SST model. Since this degradation study does not require detailed analysis of eddy formation close to the wall, the computation load was reduced by implementing wall functions that estimate the overall effects of turbulence near the wall without requiring the detailed simulation of that turbulence. A detailed description of these wall functions can be found in the OpenFOAM User Guide [3].

2.1.4. Transport Properties

All transport properties for this model are assumed to be constant throughout the calculation. While this does add some inherent error to the model, most of the properties do not change substantially over the range of temperatures present in the model. One exception is the fluid density, which is varied as a function of temperature using a constant thermal expansion coefficient. This thermal coefficient was derived from the fluid properties models used in MELCOR. The values used in this model are shown in Table 2-1 below.

Table 2-1. Transport properties used in OpenFOAM model

Property	Value
Laminar kinematic viscosity	5.295×10^{-6} m^2/s^2
Thermal expansion coefficient	2.28×10^{-4} K^{-1}
Reference Temperature	974.83 K
Laminar Prandtl Number	25.327
Turbulent Prandtl Number	0.85

2.1.5. Heat Exchanger Model Functionality

Since a full-fidelity CFD model for each of the heat exchangers used in the DRACS would require more computational cost than the rest of the model combined, it was decided to approximate the heat exchanger performance as a volumetric heat source applied directly to each control volume in the heat exchanger. The source term for each control volume was calculated by Equation [1],

$$S_{T,i} = (T_i - T_b) * \frac{h}{C_p} * V_i * dt \quad [1]$$

where

$S_{T,i}$ = Temperature Source term for control volume i,
T_i = Temperature of control volume i (K),
T_b = Bulk temperature of the interfacing fluid (K),
h = Volumetric heat transfer coefficient $\left(\frac{W}{m^3 K}\right)$,

C_P = Volumetric heat capacity $\left(\frac{kJ}{m^3K}\right)$,
V_i = Volume of control volume i (m^3),
dt = time step (s).

The interfacing fluid for the DHX is the reactor vessel salt, and the interfacing fluid for the TCHX is boiling water.

2.1.6. Reactor Vessel Response

The reactor vessel temperature is calculated by a simple energy balance at each time step as shown in Equation [2],

$$T_{vessel,new} = T_{vessel,old} + \frac{Q_{Decay} - Q_{DHX}}{C_P * V_{vessel}} \quad [2]$$

where

T = Temperature (K),

Q = Heat transferred during timestep (J),

C_P= Volumetric heat capacity $\left(\frac{kJ}{m^3K}\right)$,

V_{vessel} = Volume of salt in the reactor vessel (m^3).

Q_{Decay} is determined from interpolating linearly as a function of time between decay heat rate values provided by Oakridge National Laboratory for this reactor design. The values are tabulated in Table A-1. Q_{DHX} is calculated by summing the heat transferred to each cell in the DHX and multiplying by the number of functioning DRACS loops, with a maximum of three.

2.2. Degradation Scenarios

Three different classes of degradation scenarios were considered for this analysis. First, the possibility of some of the three available DRACS being inoperable at the time of the accident is considered. Second, situations where the DHX does not transfer heat to the DRACS loop at the expected rate are considered. Third, degradation of the TCHX is considered, where heat removal is decreased for an unspecified reason.

2.2.1. DRACS Loop Failures

The DRACS loop failure scenario is implemented by adjusting the value of Q_{DHX} dependent on the number of available DRACS loops. The full performance situation features three DRACS loops. Two degraded scenarios using two and one DRACS loops are also considered. The case where all three DRACS loops are unavailable is neglected since the OpenFOAM model will have no effect on the reactor vessel temperature in such a scenario.

2.2.2. DRACS Loop degradation

Two forms of DRACS loop degradation are considered. First, a decreased performance of the DHX, limiting the rate that heat is removed from the reactor vessel. Second, decreased performance of the TCHX, which leads to higher salt loop temperatures, ultimately decreasing the rate heat is removed from the reactor vessel. Heat exchanger degradation is modeled identically in both cases, by adjusting the heat transfer coefficient used to calculate heat transferred into or out of each cell in the heat exchanger.

2.3. Test Matrix

Twenty-one different calculations were performed as part of this study. One calculation investigated the DRACS performance if all three DRACS loops were available and operating at full capacity, along with twenty different degradation scenarios. Two of these scenarios investigated the total failure of one or two DRACS loops, and the others investigated the effects of partial performance degradation of each heat exchanger in the DRACS loop. For the eighteen DRACS loop degradation scenarios, it was assumed all three DRACS loops were available. Scenario descriptions for each scenario are presented in Table 2-2.

Table 2-2. Test Matrix

Scenario #	Available DRACS Loops	% Capacity of DHX	% Capacity of TCHX
1	3	100	100
2	2	100	100
3	1	100	100
4	3	90	100
5	3	80	100
6	3	70	100
7	3	60	100
8	3	50	100
9	3	40	100
10	3	30	100
11	3	20	100
12	3	10	100
13	3	100	90
14	3	100	80

Scenario #	Available DRACS Loops	% Capacity of DHX	% Capacity of TCHX
15	3	100	70
16	3	100	60
17	3	100	50
18	3	100	40
19	3	100	30
20	3	100	20
21	3	100	10

3. RESULTS

To evaluate the effect of different degradation scenarios, the results of each test will be presented for comparison in the following ways:

- The maximum reactor temperature reached
- The maximum temperature reached in the DRACS hot leg
- The time taken for the reactor temperature to fall below the operation temperature
- A plot of heat transfer rate over time for each heat exchanger
- A plot of the reactor vessel temperature over time
- A picture of the temperature distribution in the DRACS loop 1 hour after the accident begins

After presenting the results from each test, a summary of results will be shown in Table 3-1.

3.1. DRACS Loop Failures

Scenarios #1-#3 investigate the overall effect on the reactor vessel assuming one or more of the DRACS loops becomes unavailable at the time of the accident. All three cases begin at steady state assuming a constant reactor vessel temperature of 973 K.

3.1.1. Scenario #1

Scenario #1 models the DRACS performance when all three DRACS loops are fully operational. The maximum temperature reached was 975.8 K. Reactor first returns to operational temperature 305 seconds after the accident begins.

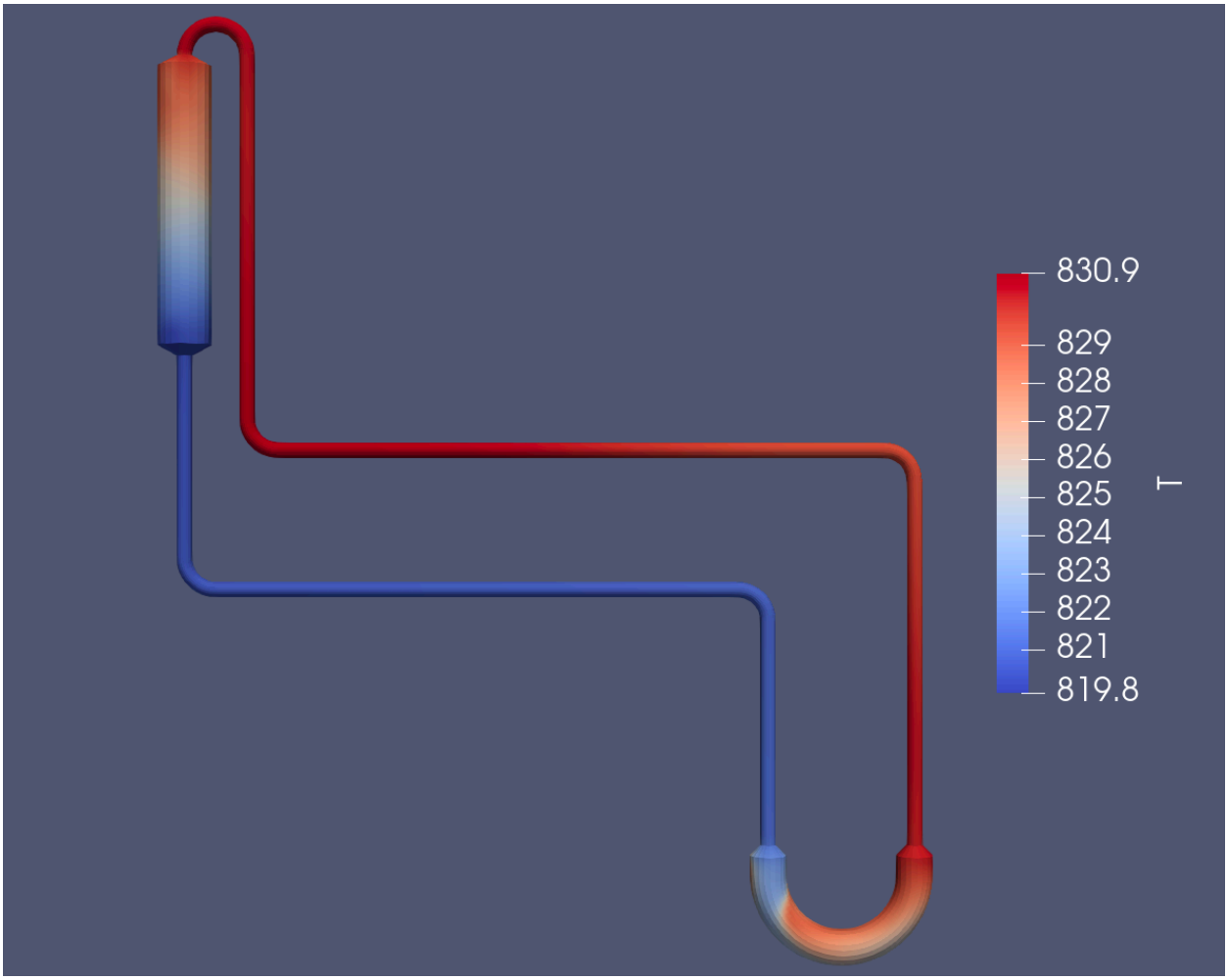

Figure 3-1. Scenario #1 Dracs loop temperature distribution one hour after the accident.

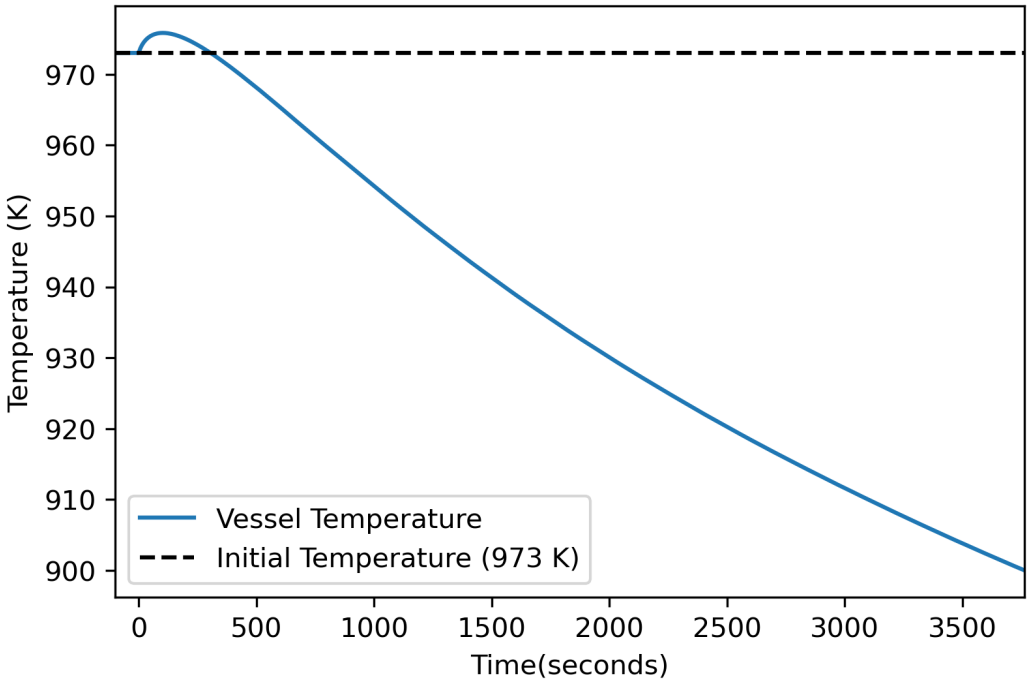

Figure 3-2. Scenario #1 Reactor Vessel Temperature

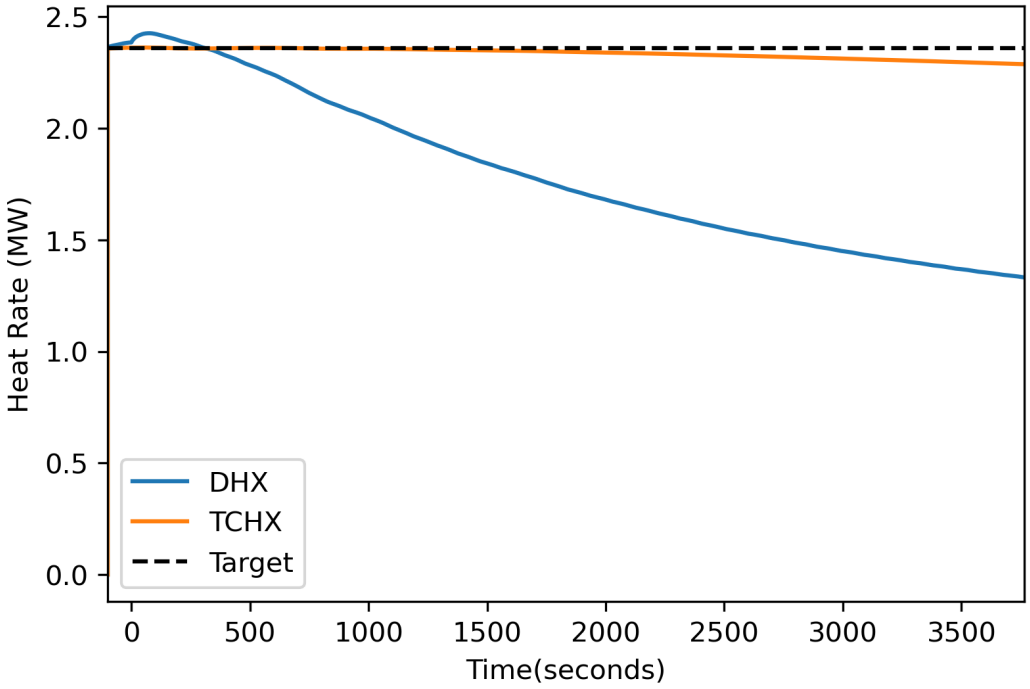

Figure 3-3. Scenario #1 Heat Exchanger heat removal rates

3.1.2. Scenario #2

Scenario #2 models the DRACS performance when two DRACS loops are fully operational. The maximum temperature reached was 986.8 K. Reactor first returns to operational temperature 1980 seconds after the accident begins.

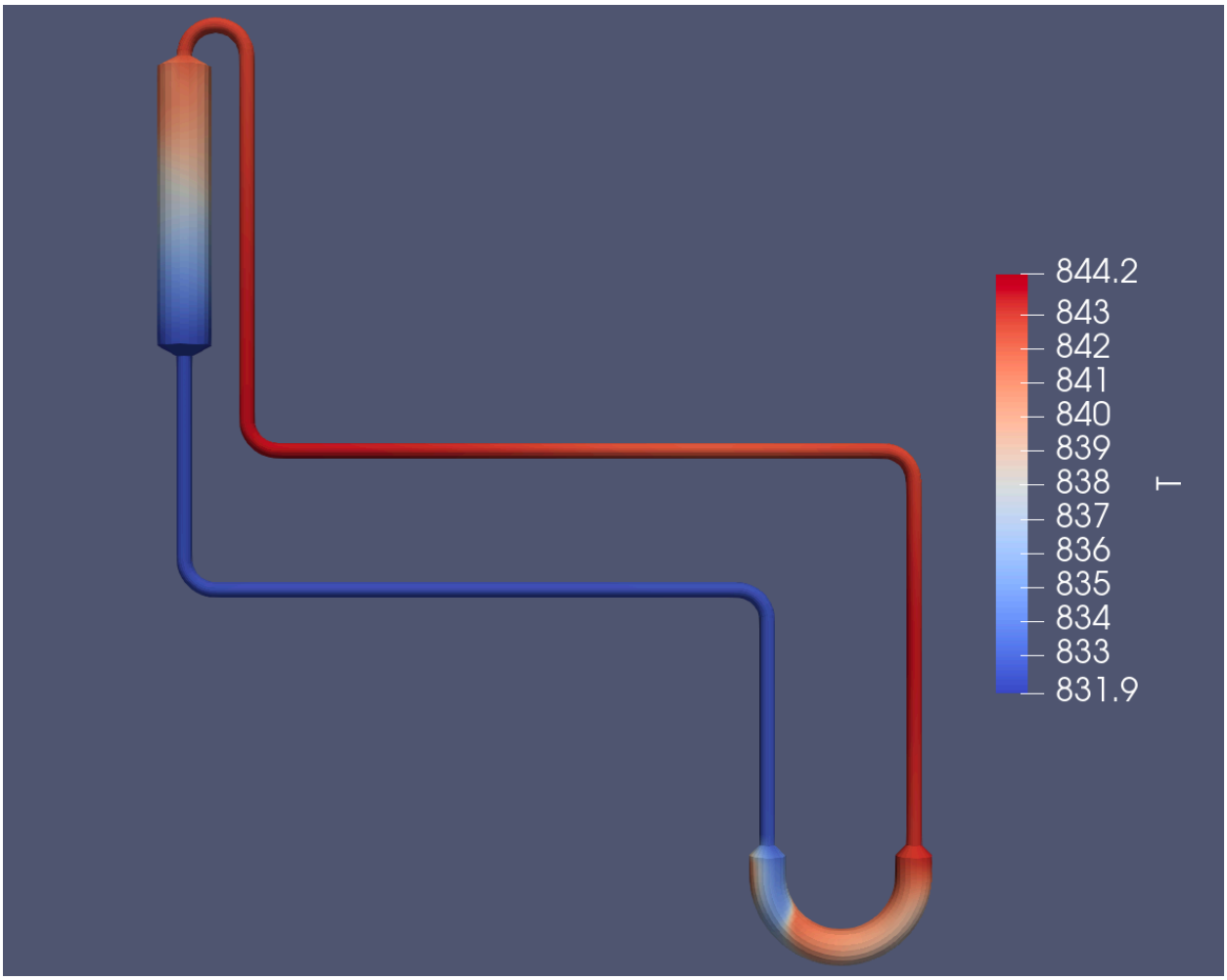

Figure 3-4. Scenario #2 Dracs loop temperature distribution one hour after the accident.

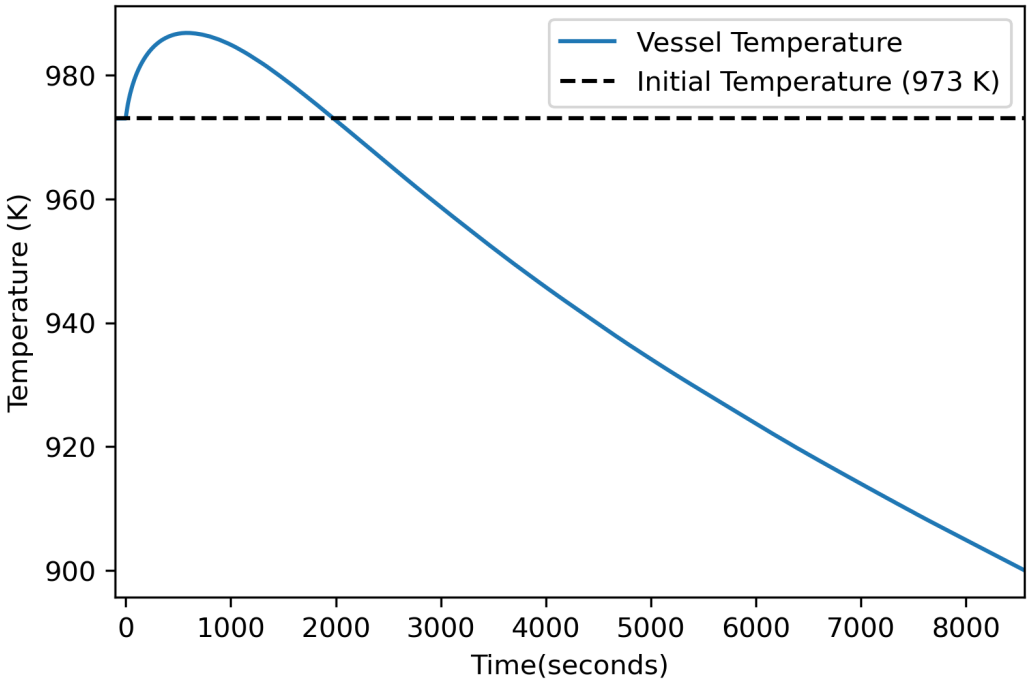

Figure 3-5. Scenario #2 Reactor Vessel Temperature

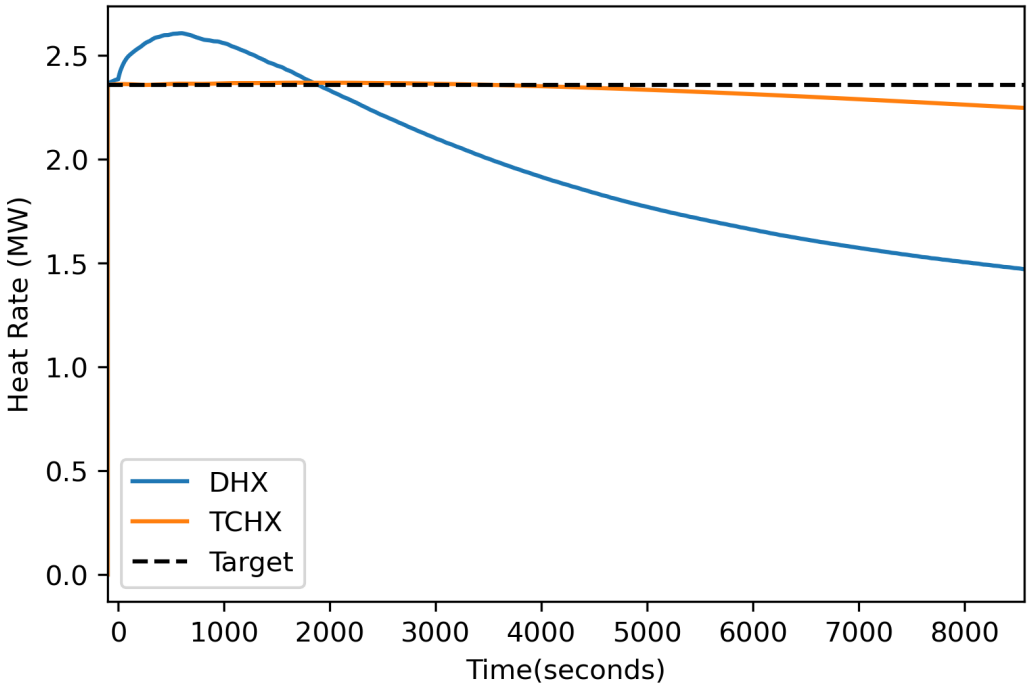

Figure 3-6. Scenario #2 Heat Exchanger heat removal rates

3.1.3. Scenario #3

Scenario #3 models the DRACS performance when only one DRACS loops is operational. The maximum temperature reached was 1046.1 K. After four hours, the reactor temperature was decreasing, but was still above the operational temperature. The calculation was ended early due to computational time constraints.

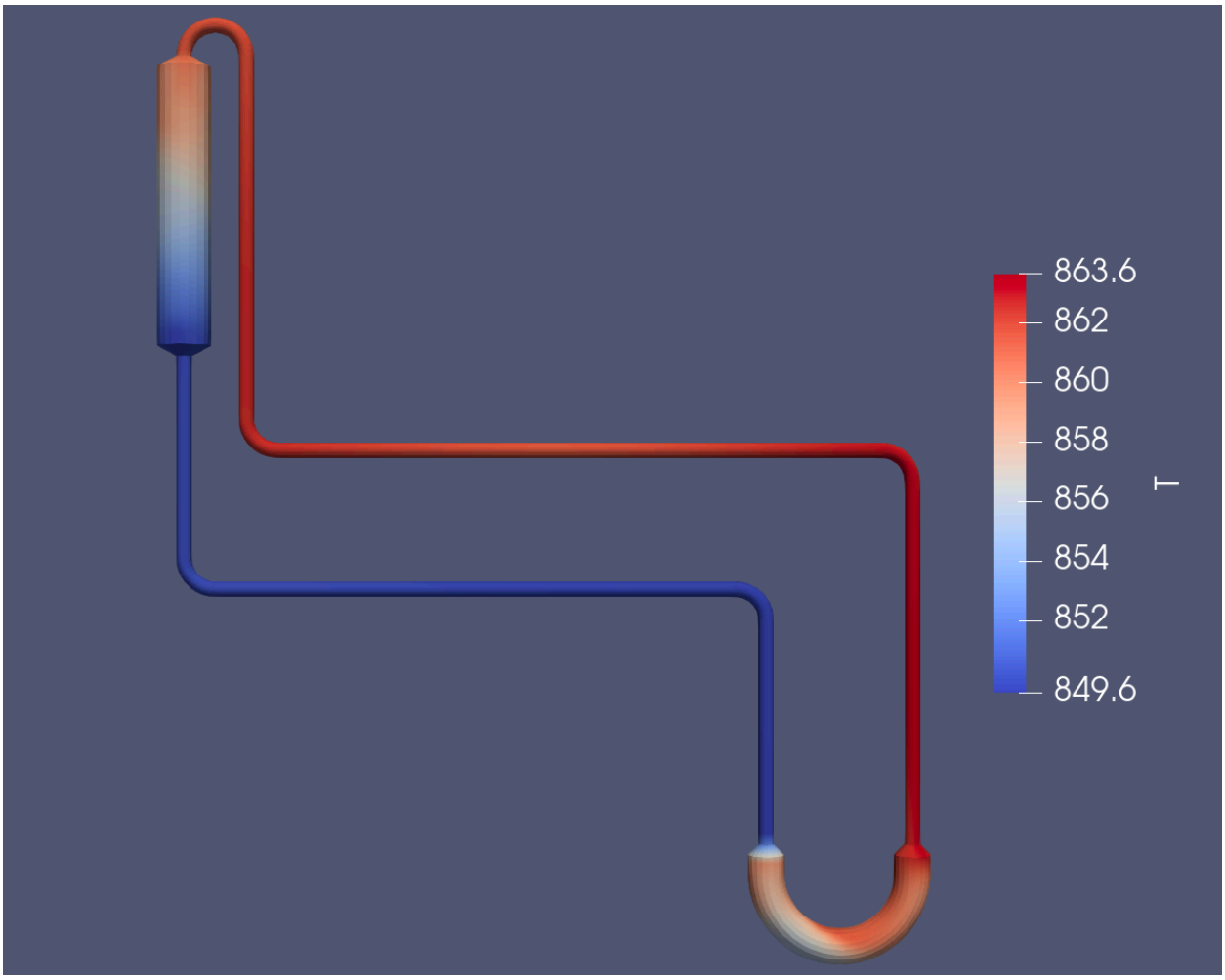

Figure 3-7. Scenario #3 Dracs loop temperature distribution one hour after the accident.

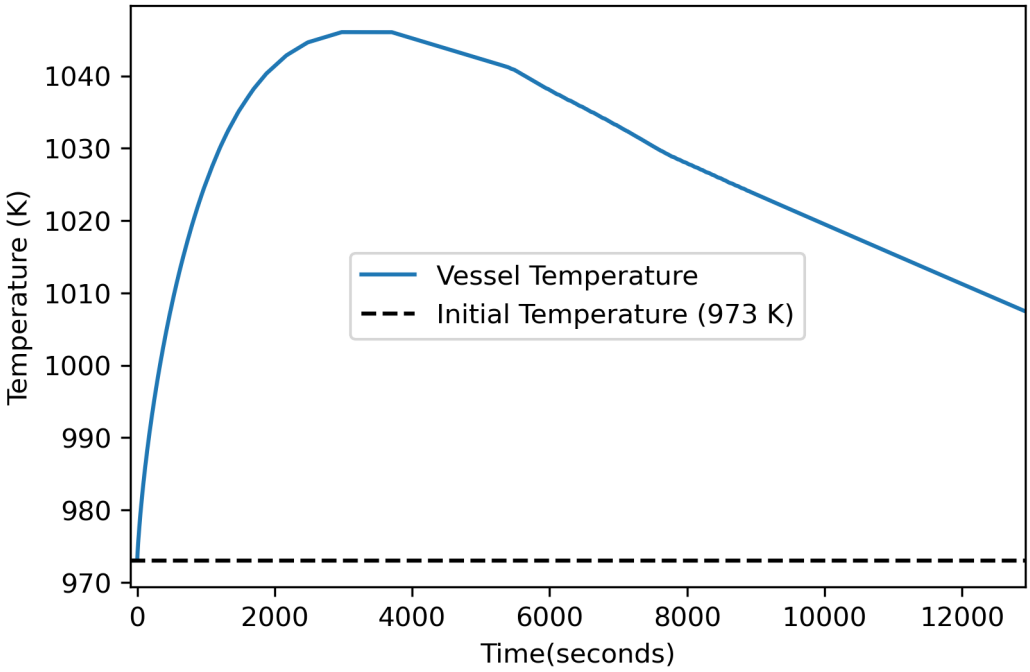

Figure 3-8. Scenario #3 Reactor Vessel Temperature

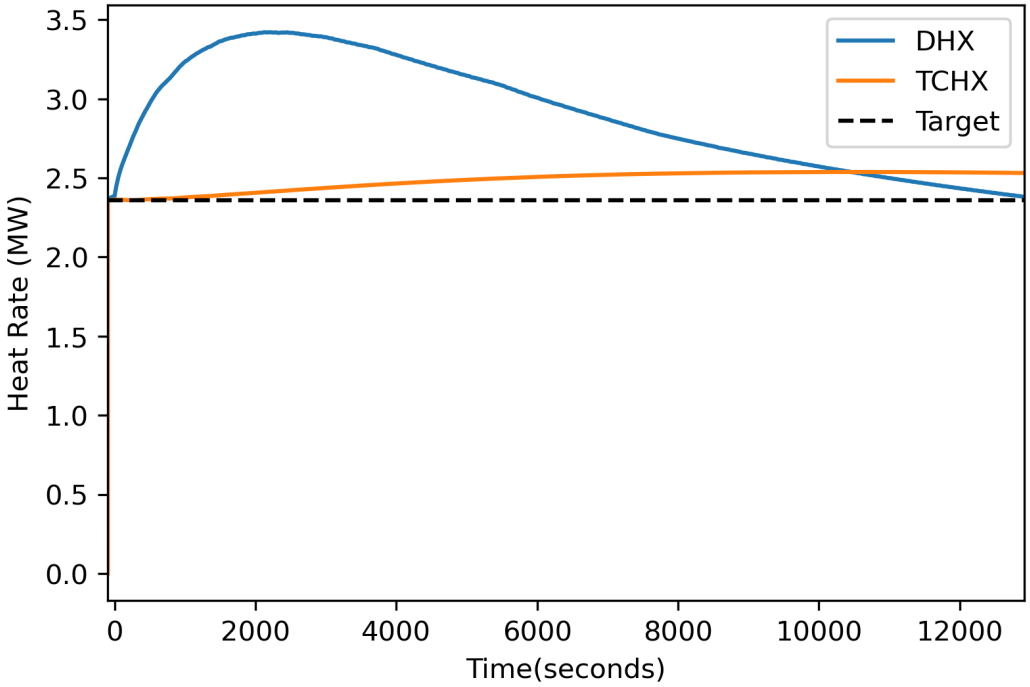

Figure 3-9. Scenario #3 Heat Exchanger heat removal rates

3.2. DHX Degradation Scenarios

Scenarios #4-#12 investigate the effects of degraded DHX performance. For these cases, it is assumed all three DRACS loops perform identically, and that DHX performance degrades instantaneously at the start of the accident following 100 seconds of steady state operation.

3.2.1. Scenario #4

Scenario #4 models the DRACS performance when all three DRACS loops are available, with the DHX operating at 90% capacity. The maximum temperature reached was 977.4 K. Reactor first returns to operational temperature 510 seconds after the accident begins.

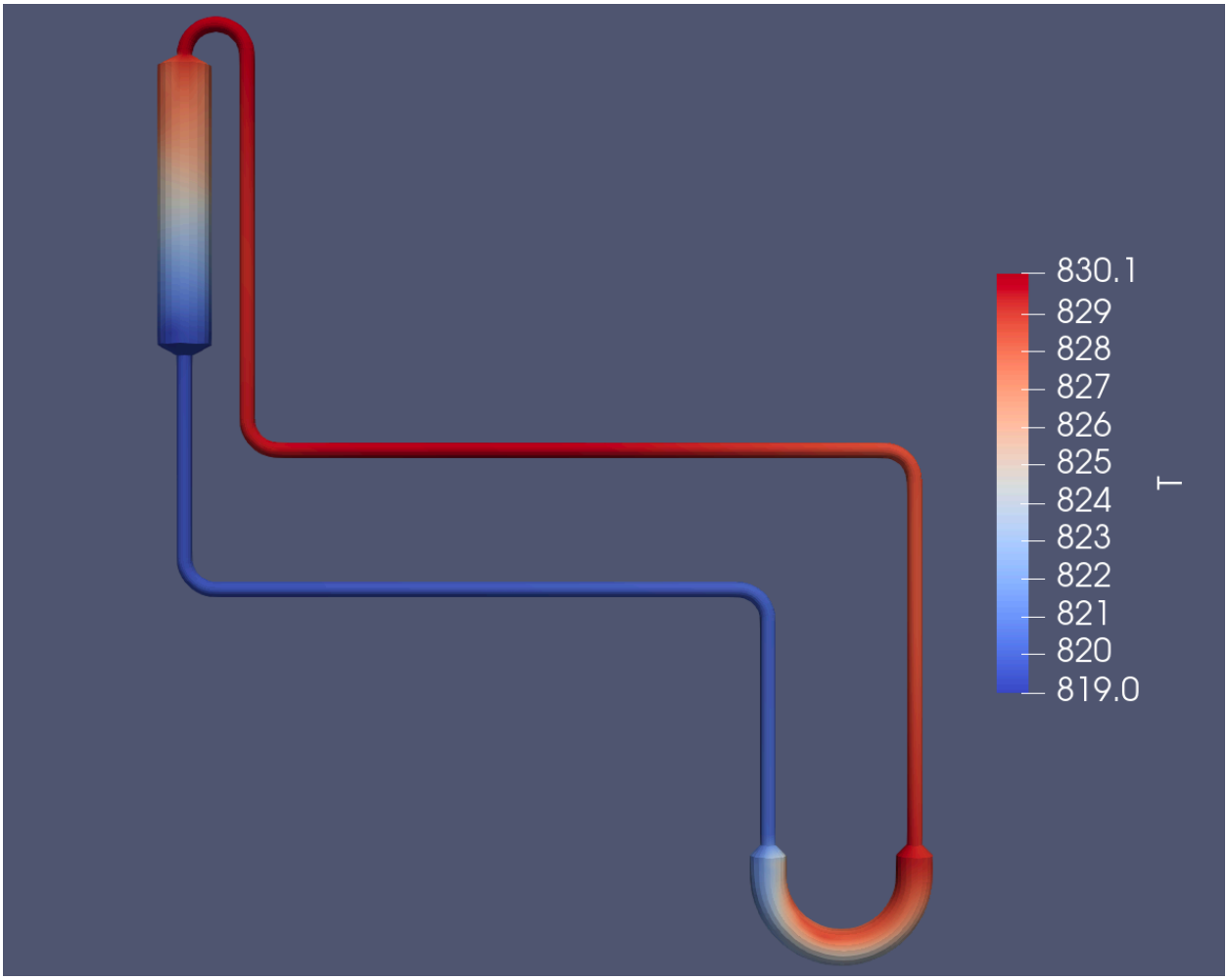

Figure 3-10. Scenario #4 Dracs loop temperature distribution one hour after the accident.

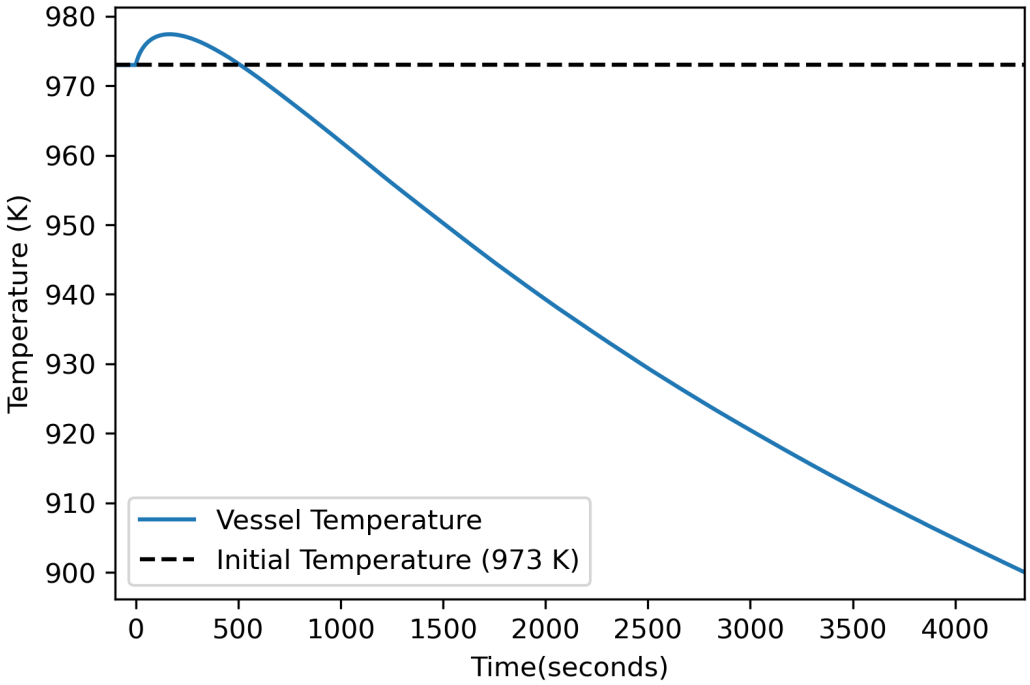

Figure 3-11. Scenario #4 Reactor Vessel Temperature

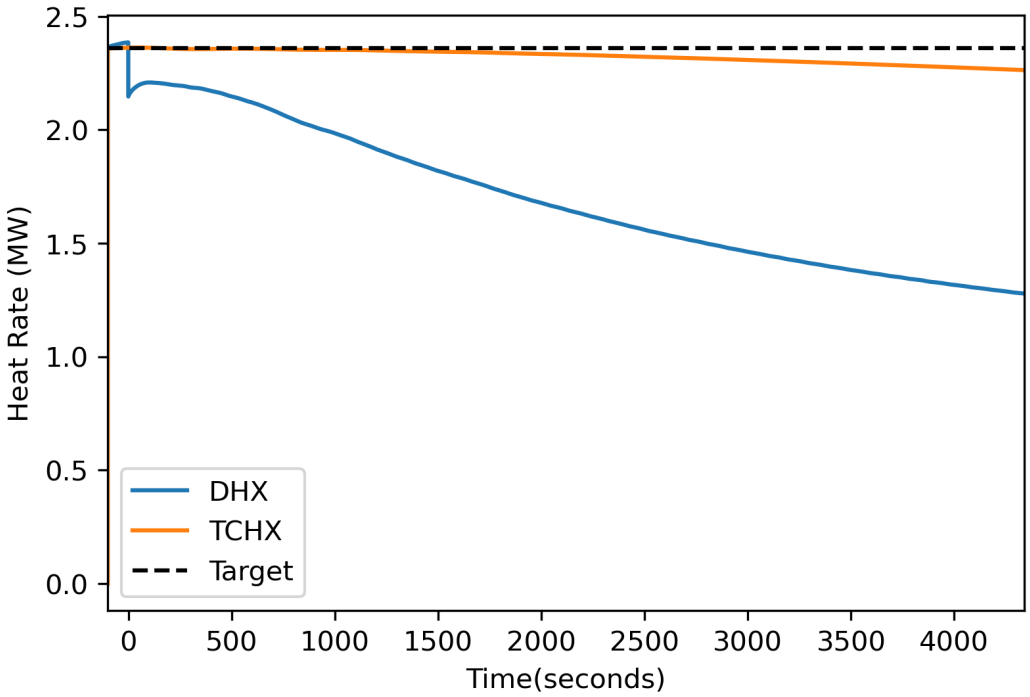

Figure 3-12. Scenario #4 Heat Exchanger heat removal rates

3.2.2. Scenario #5

Scenario #5 models the DRACS performance when all three DRACS loops are available, with the DHX operating at 80% capacity. The maximum temperature reached was 980.0 K. Reactor first returns to operational temperature 866 seconds after the accident begins.

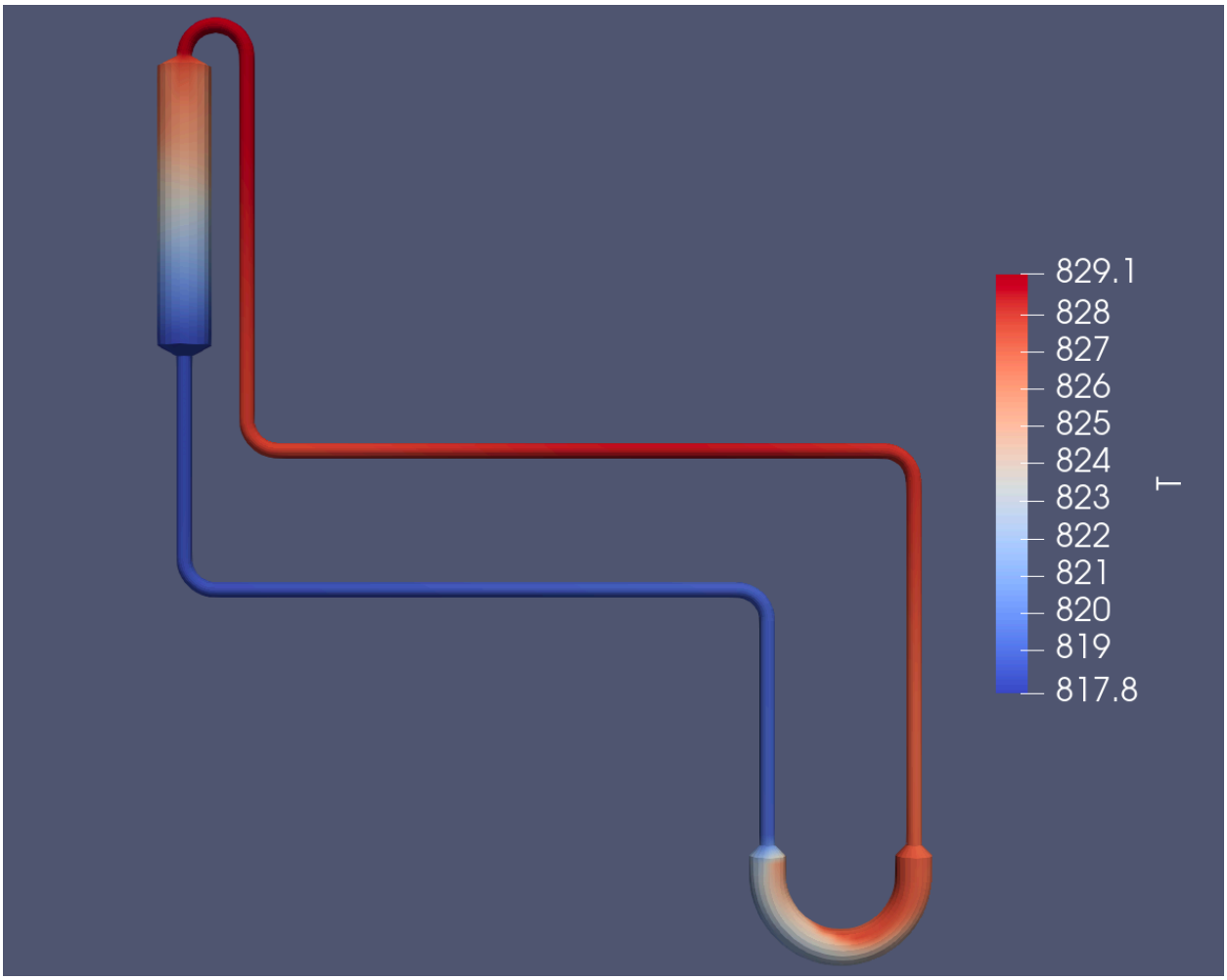

Figure 3-13. Scenario #5 Dracs loop temperature distribution one hour after the accident.

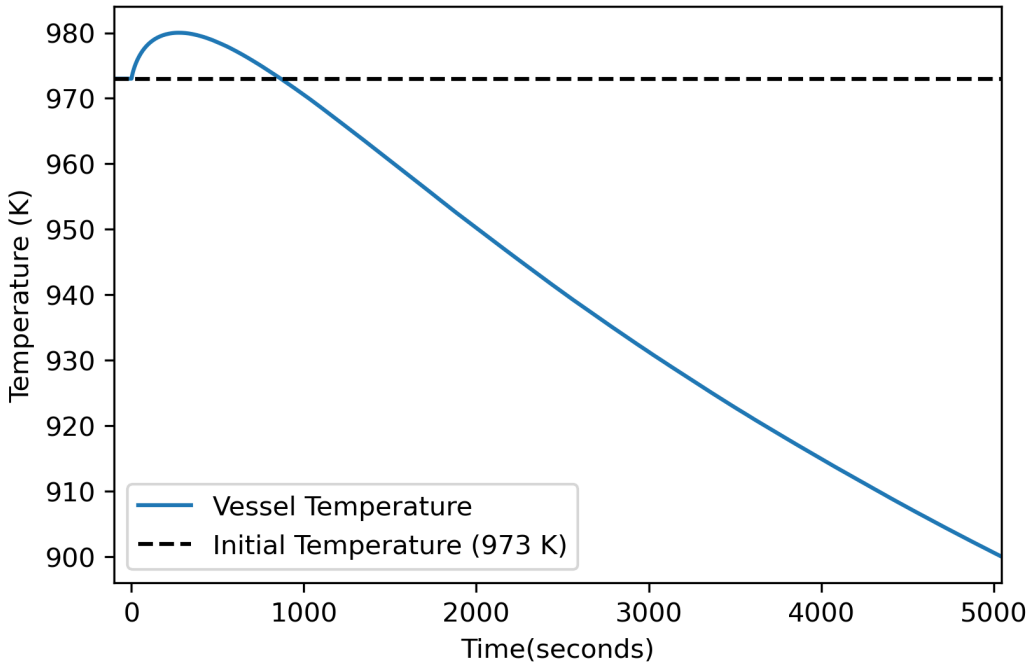

Figure 3-14. Scenario #5 Reactor Vessel Temperature

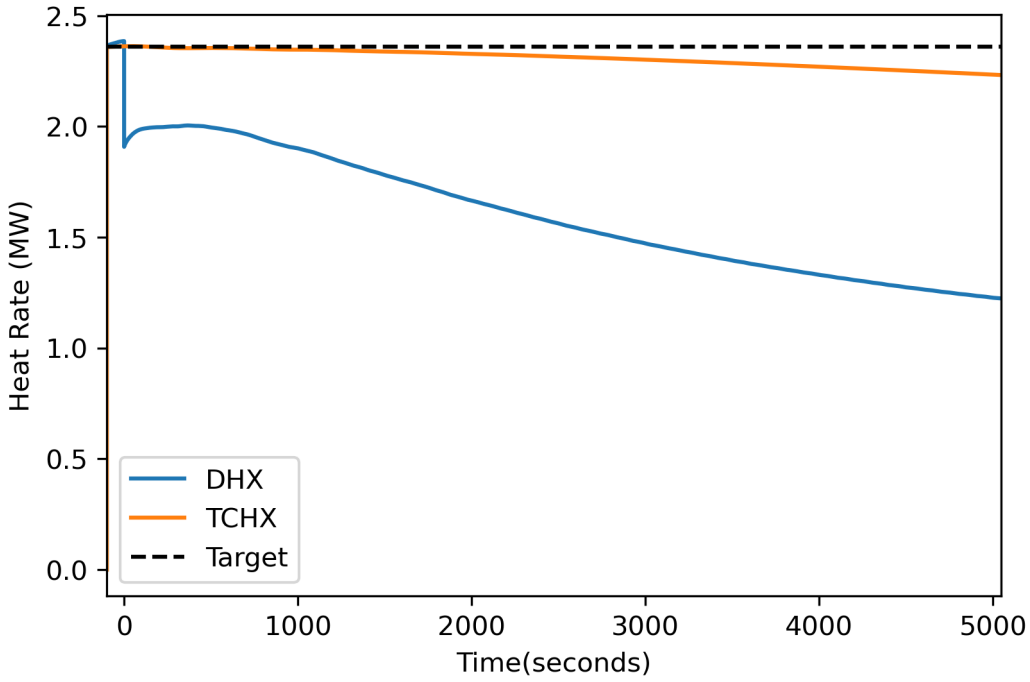

Figure 3-15. Scenario #5 Heat Exchanger heat removal rates

3.2.3. Scenario #6

Scenario #6 models the DRACS performance when all three DRACS loops are available, with the DHX operating at 70% capacity. The maximum temperature reached was 984.3 K. Reactor first returns to operational temperature 1446 seconds after the accident begins.

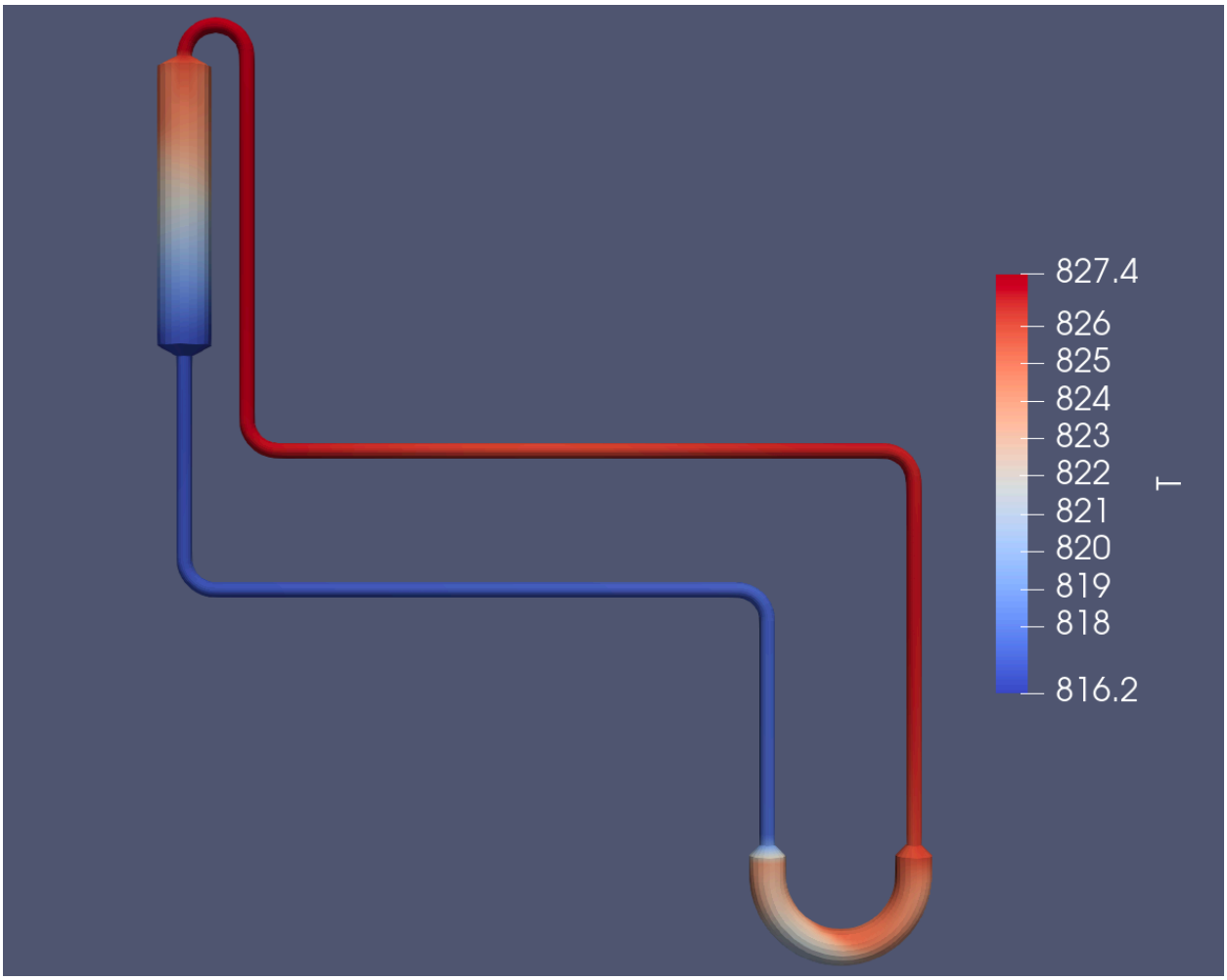

Figure 3-16. Scenario #6 Dracs loop temperature distribution one hour after the accident.

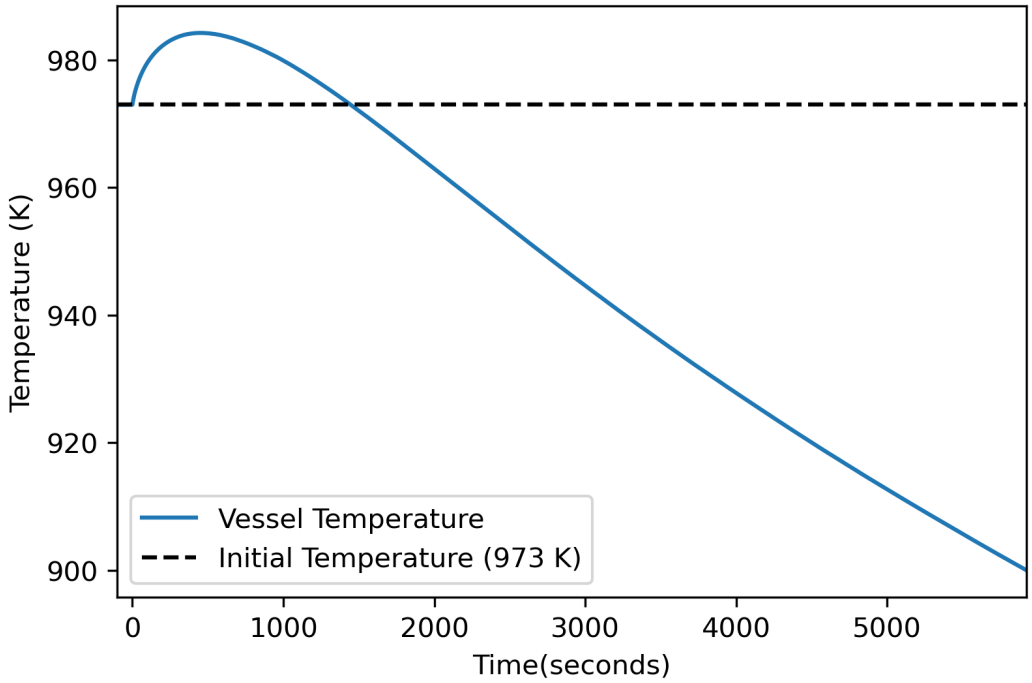

Figure 3-17. Scenario #6 Reactor Vessel Temperature

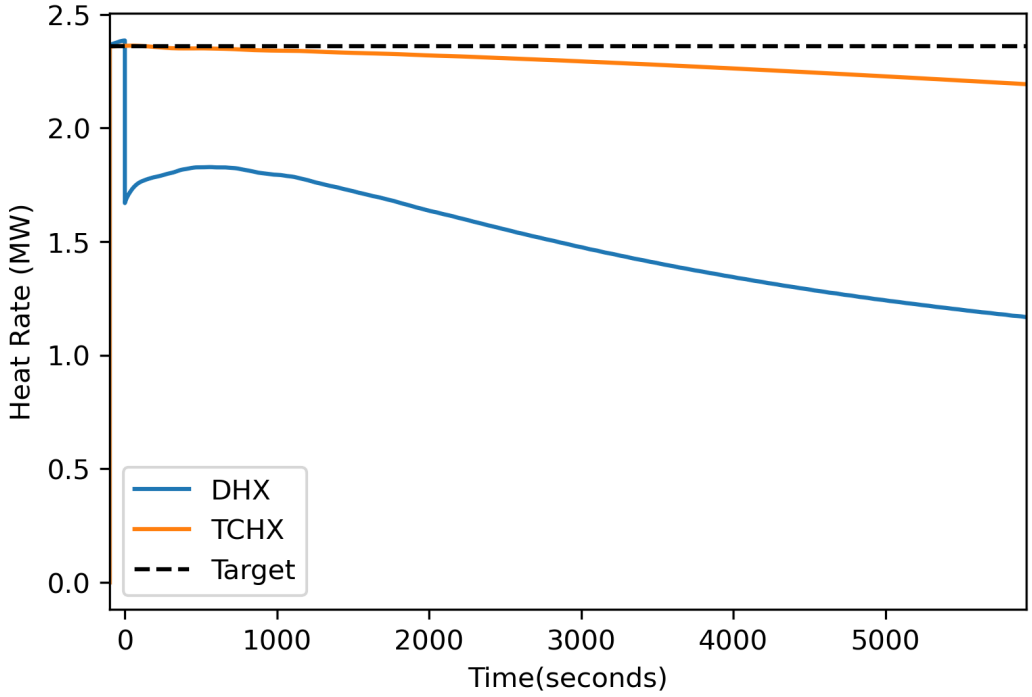

Figure 3-18. Scenario #6 Heat Exchanger heat removal rates

3.2.4. Scenario #7

Scenario #7 models the DRACS performance when all three DRACS loops are available, with the DHX operating at 60% capacity. The maximum temperature reached was 991.0 K. Reactor first returns to operational temperature 2309 seconds after the accident begins.

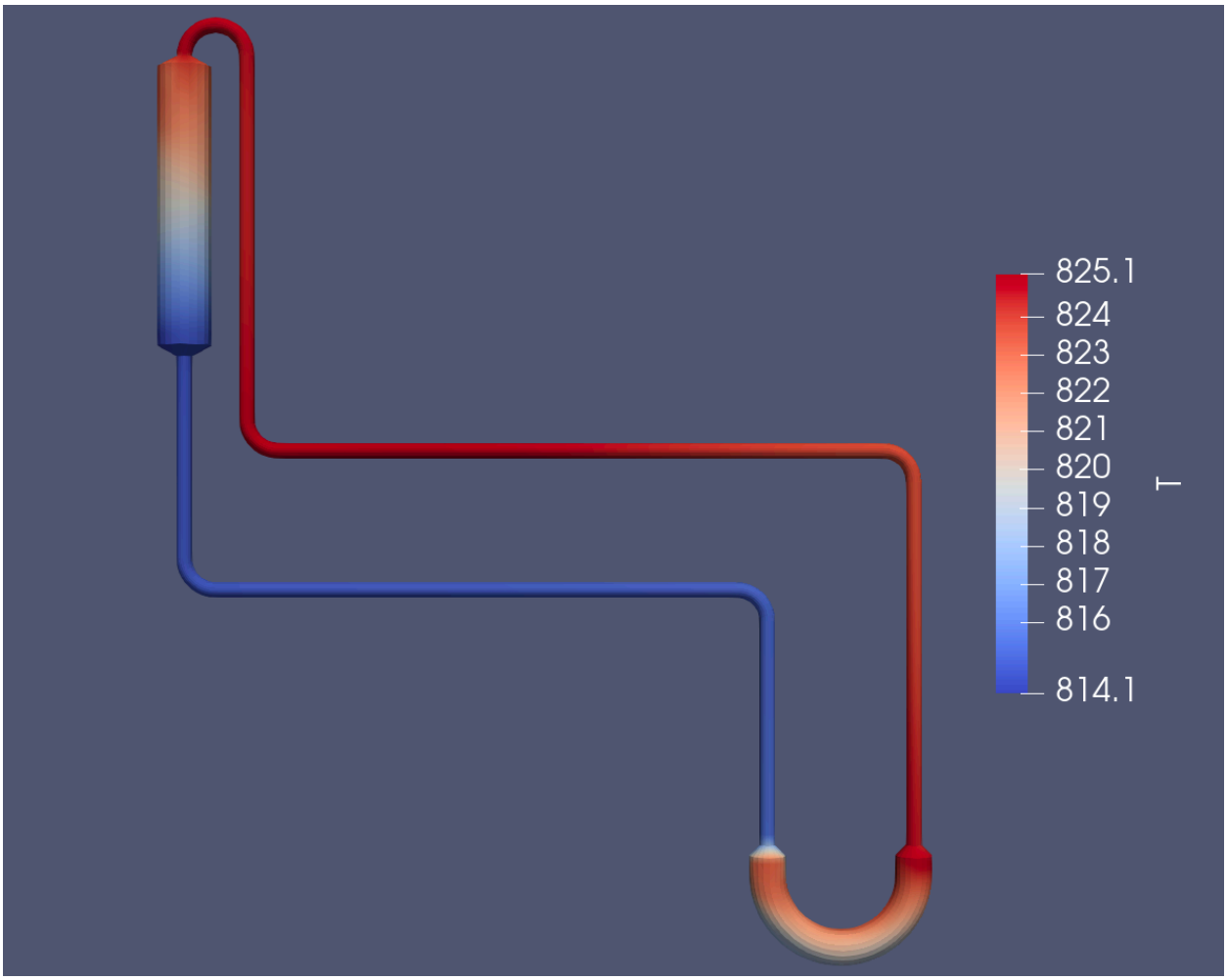

Figure 3-19. Scenario #7 Dracs loop temperature distribution one hour after the accident.

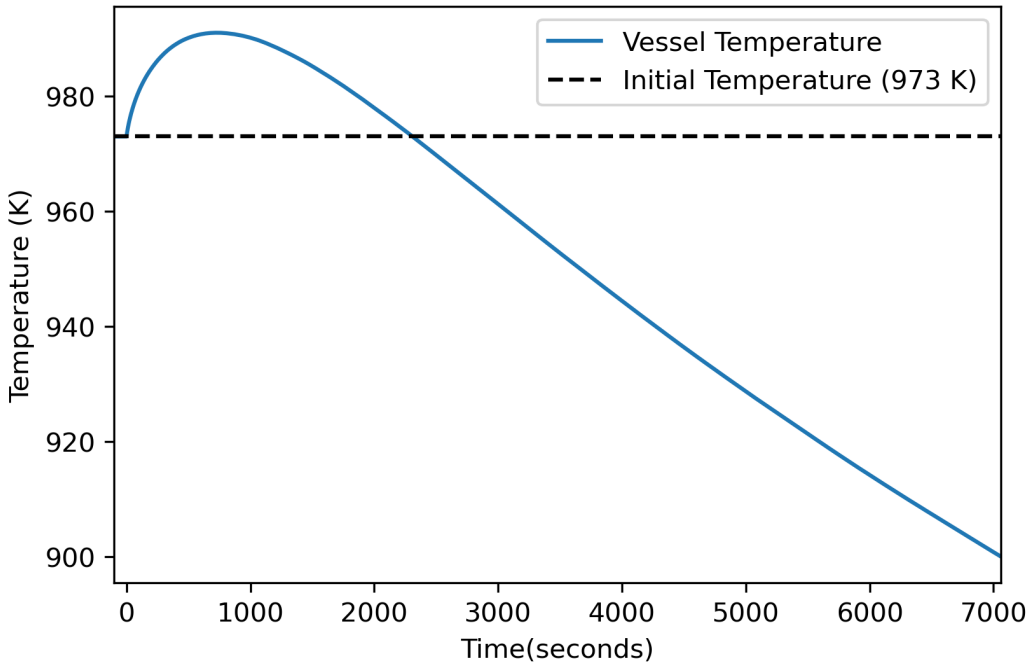

Figure 3-20. Scenario #7 Reactor Vessel Temperature

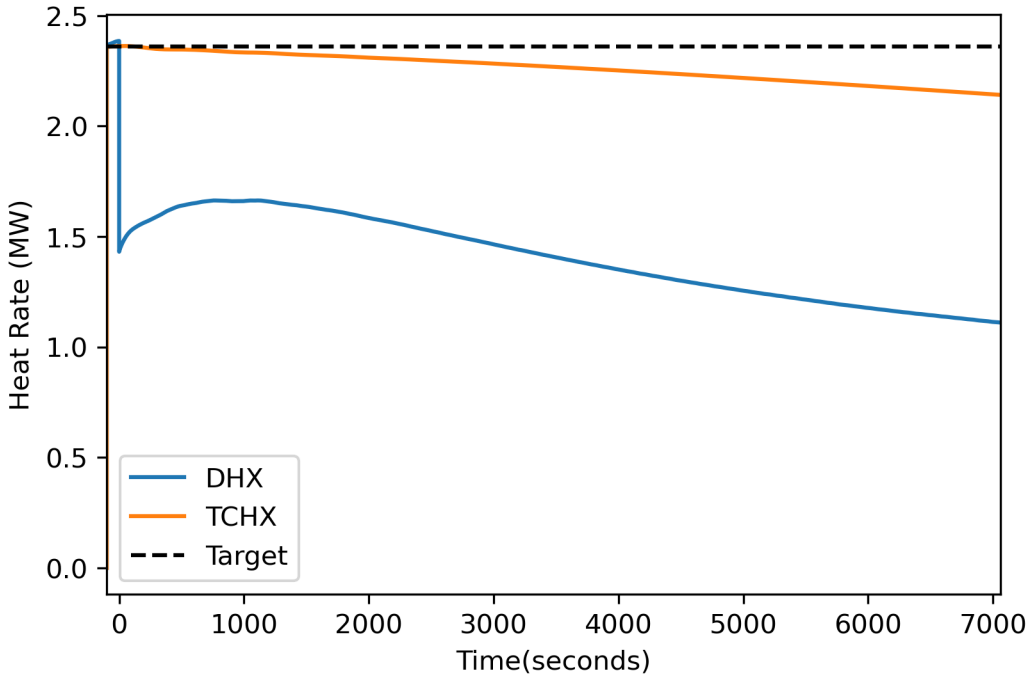

Figure 3-21. Scenario #7 Heat Exchanger heat removal rates

3.2.5. Scenario #8

Scenario #8 models the DRACS performance when all three DRACS loops are available, with the DHX operating at 50% capacity. The maximum temperature reached was 1001.6 K. Reactor first returns to operational temperature 3586 seconds after the accident begins.

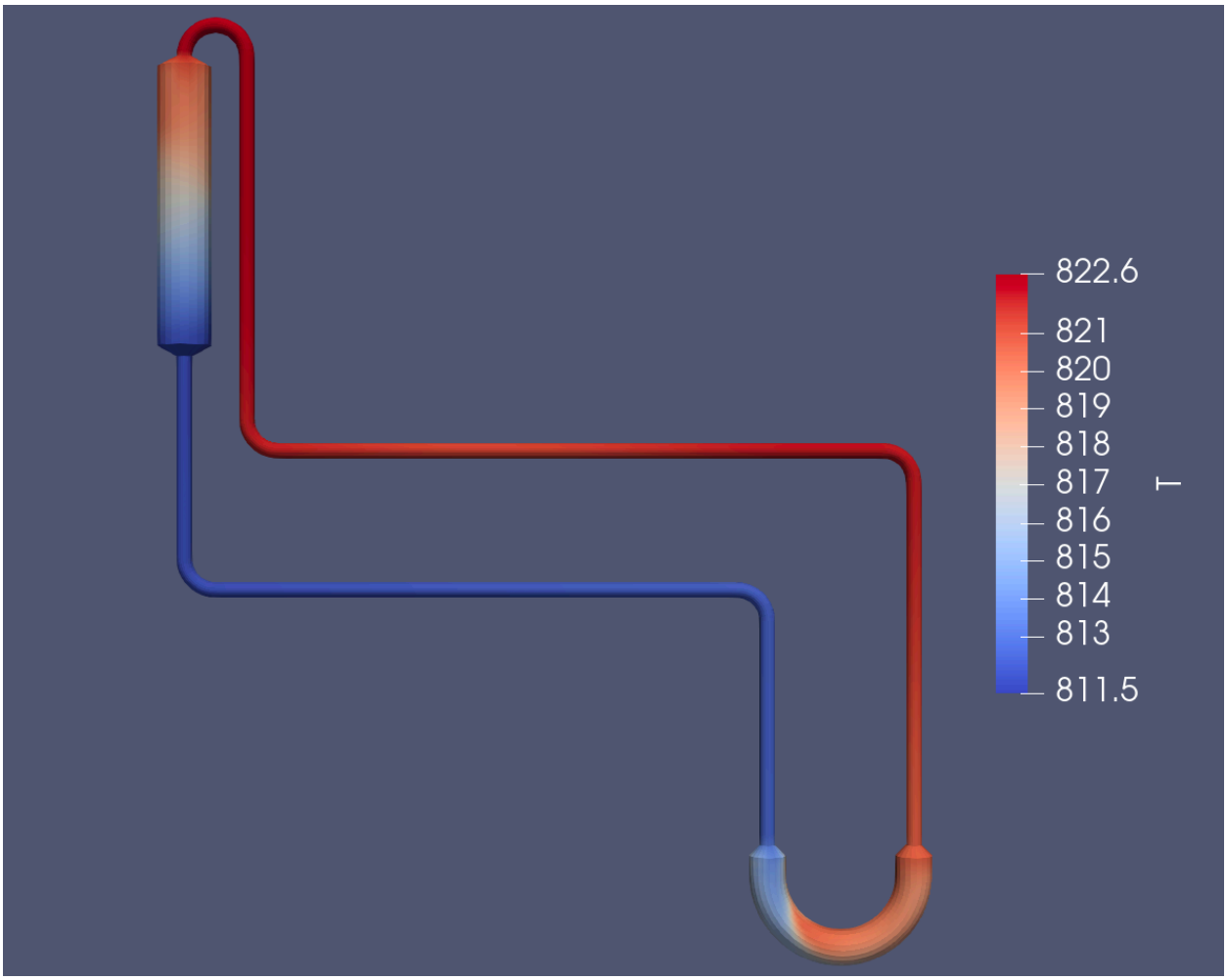

Figure 3-22. Scenario #8 Dracs loop temperature distribution one hour after the accident.

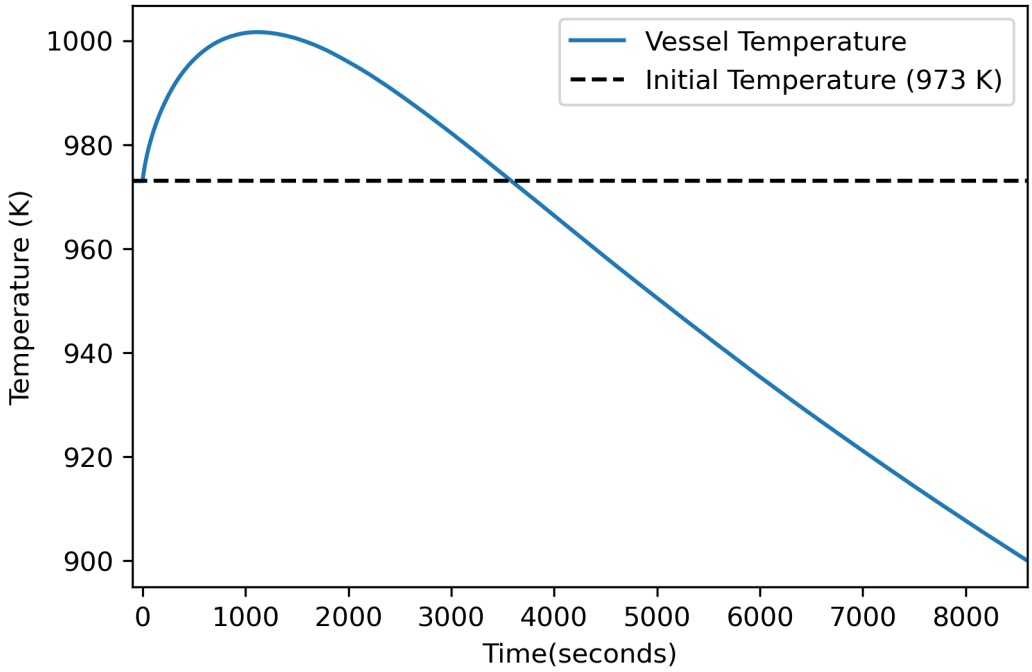

Figure 3-23. Scenario #8 Reactor Vessel Temperature

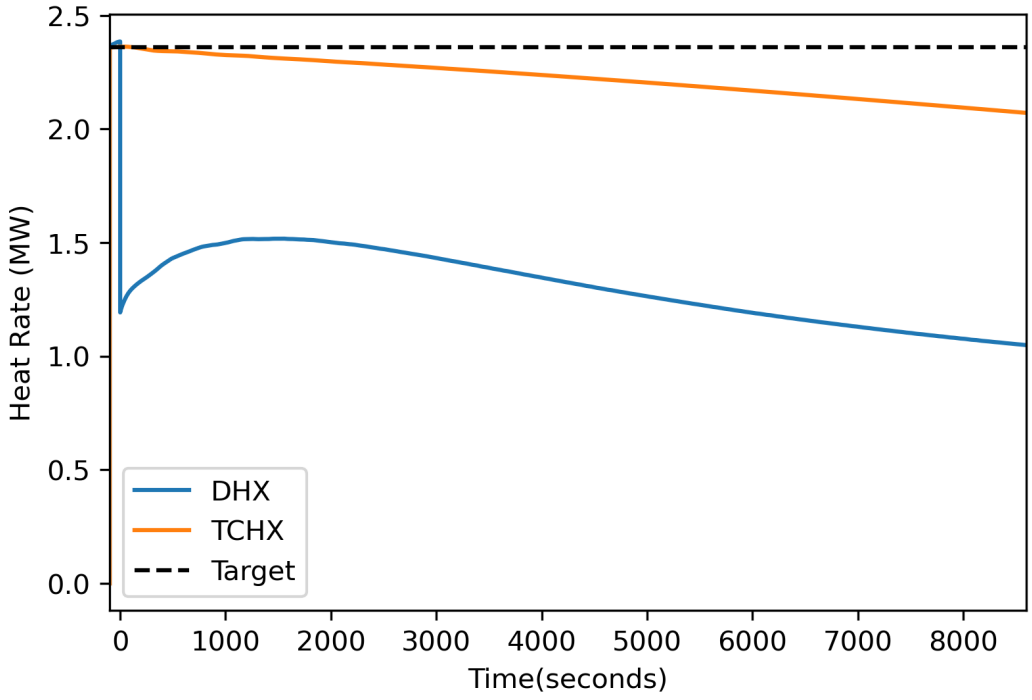

Figure 3-24. Scenario #8 Heat Exchanger heat removal rates

3.2.6. Scenario #9

Scenario #9 models the DRACS performance when all three DRACS loops are available, with the DHX operating at 40% capacity. The maximum temperature reached was 1018.0 K. Reactor first returns to operational temperature 5524 seconds after the accident begins.

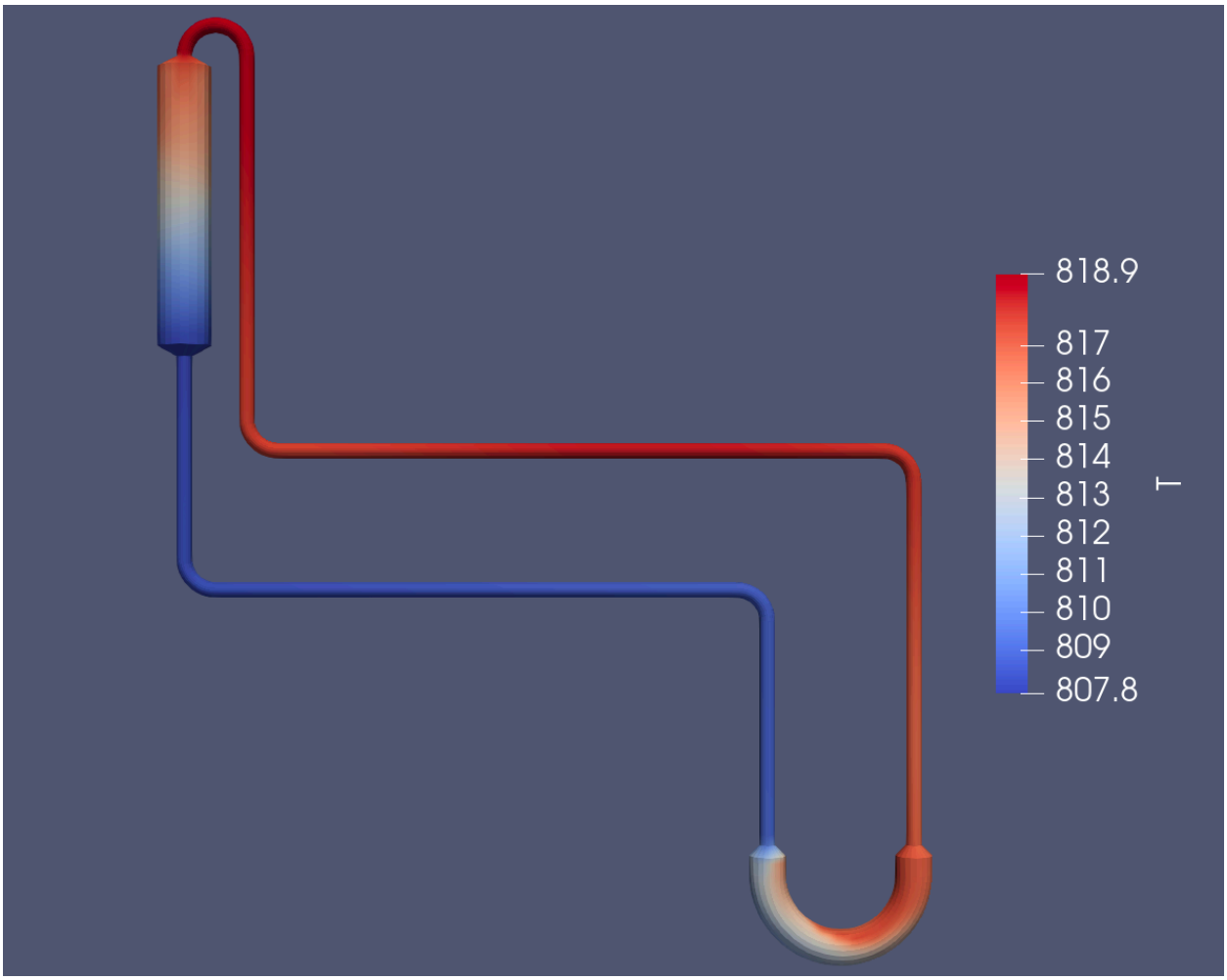

Figure 3-25. Scenario #9 Dracs loop temperature distribution one hour after the accident.

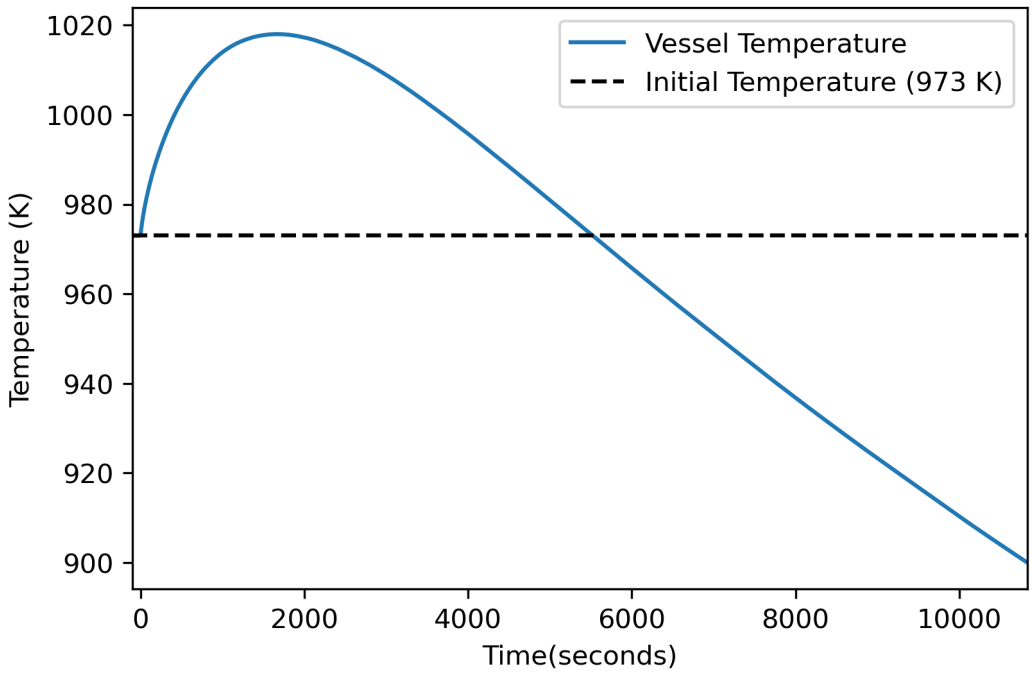

Figure 3-26. Scenario #9 Reactor Vessel Temperature

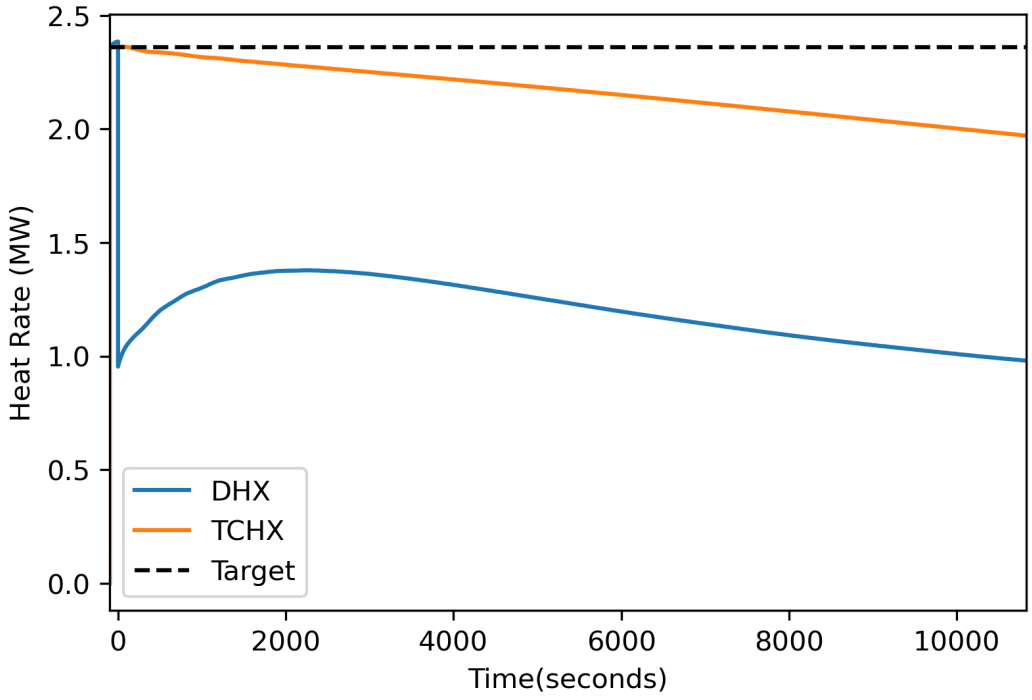

Figure 3-27. Scenario #9 Heat Exchanger heat removal rates

3.2.7. Scenario #10

Scenario #10 models the DRACS performance when all three DRACS loops are available, with the DHX operating at 30% capacity. The maximum temperature reached was 1044.2 K. Reactor first returns to operational temperature 8714 seconds after the accident begins.

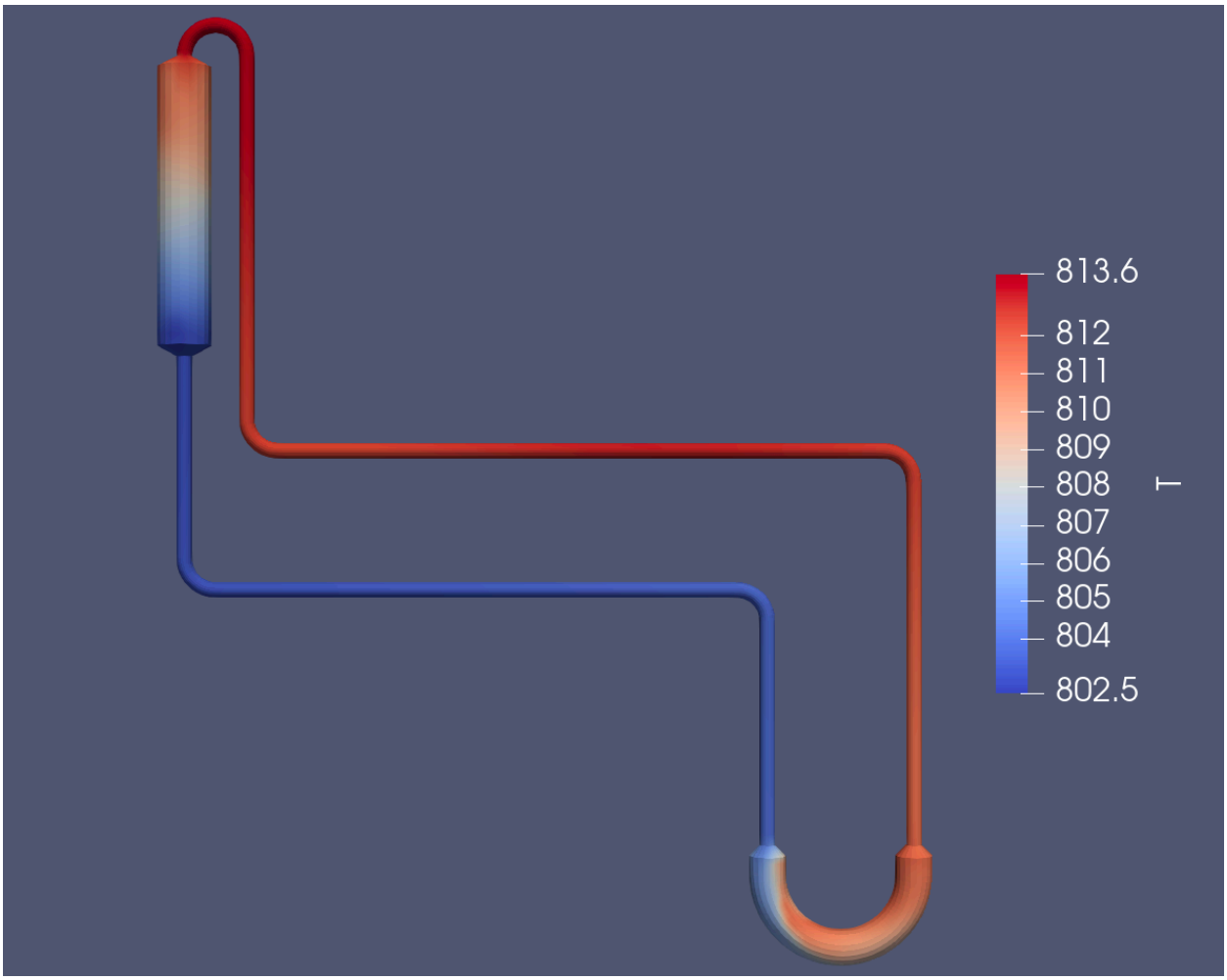

Figure 3-28. Scenario #10 Dracs loop temperature distribution one hour after the accident.

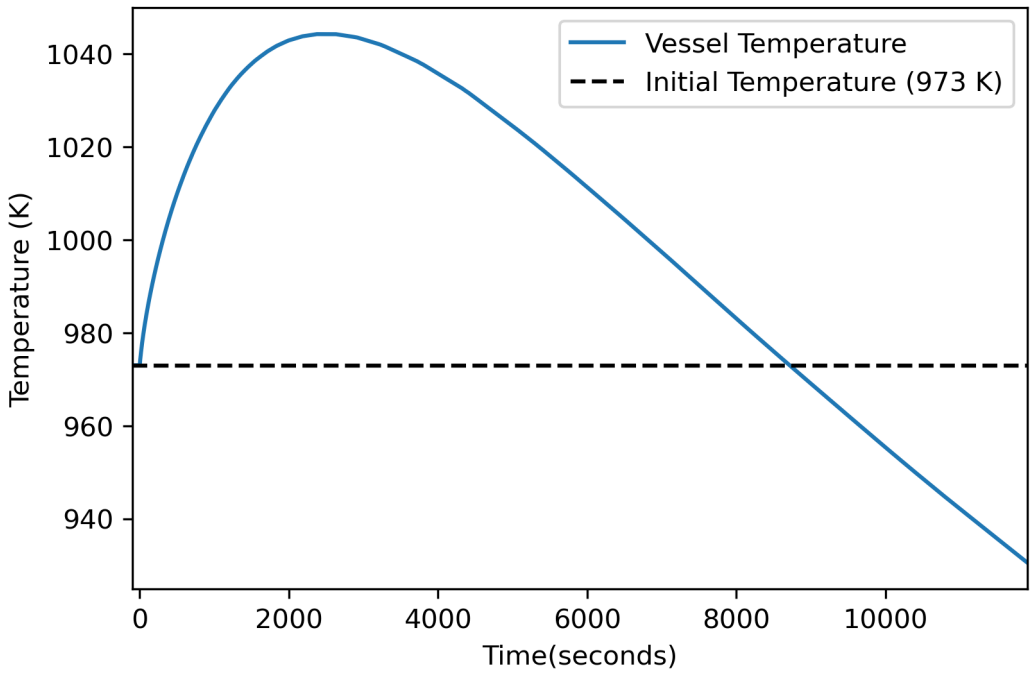

Figure 3-29. Scenario #10 Reactor Vessel Temperature

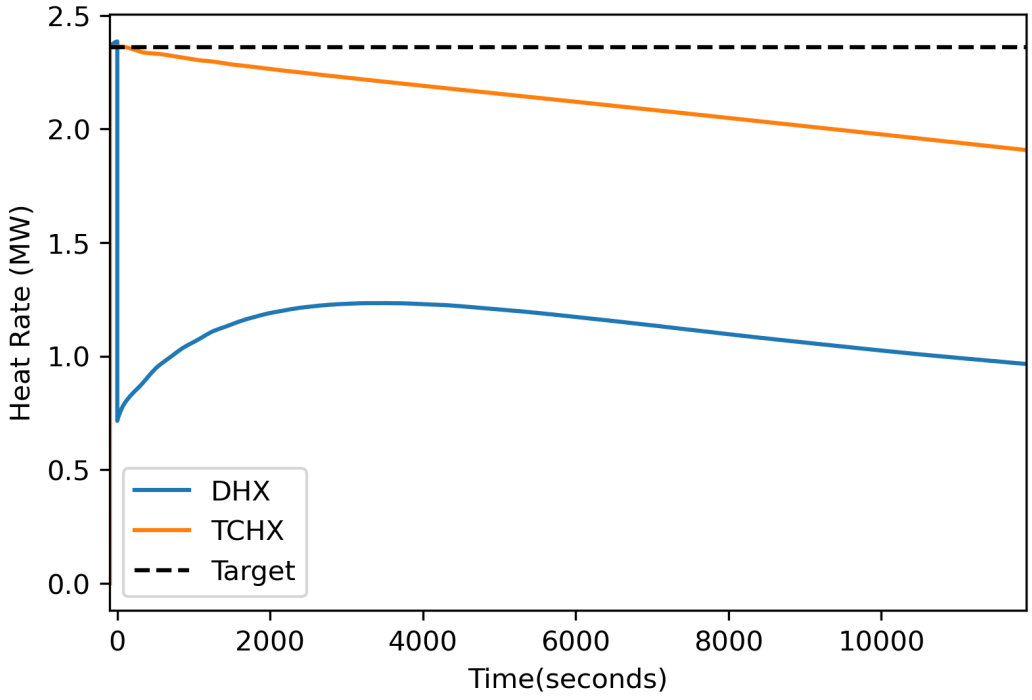

Figure 3-30. Scenario #10 Heat Exchanger heat removal rates

3.2.8. Scenario #11

Scenario #11 models the DRACS performance when all three DRACS loops are available, with the DHX operating at 20% capacity. The maximum temperature reached was 1091.4 K. After 3.3 hours, the reactor temperature was decreasing, but had not yet reached the operational temperature. The simulation was ended early due to computation time limits.

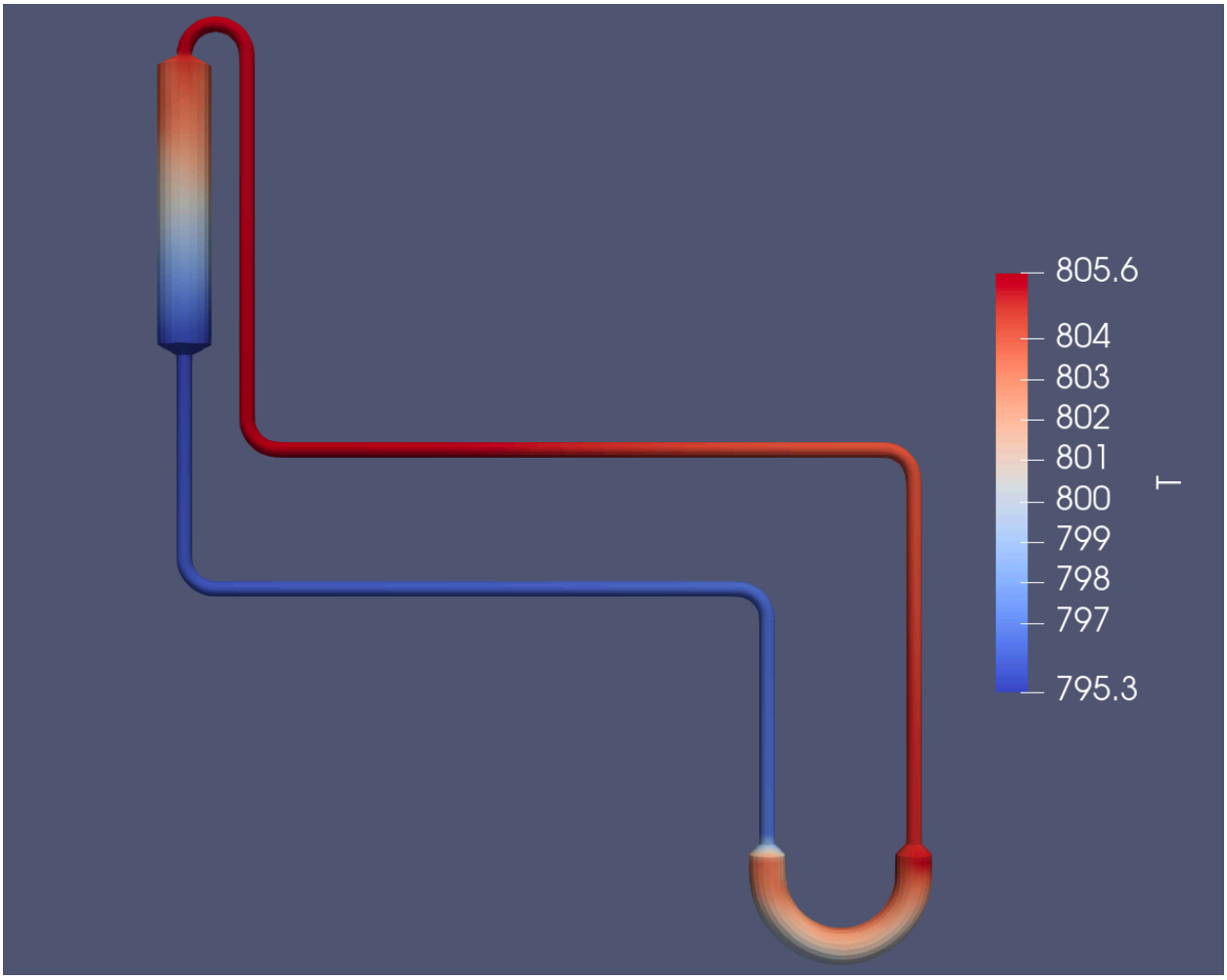

Figure 3-31. Scenario #11 Dracs loop temperature distribution one hour after the accident.

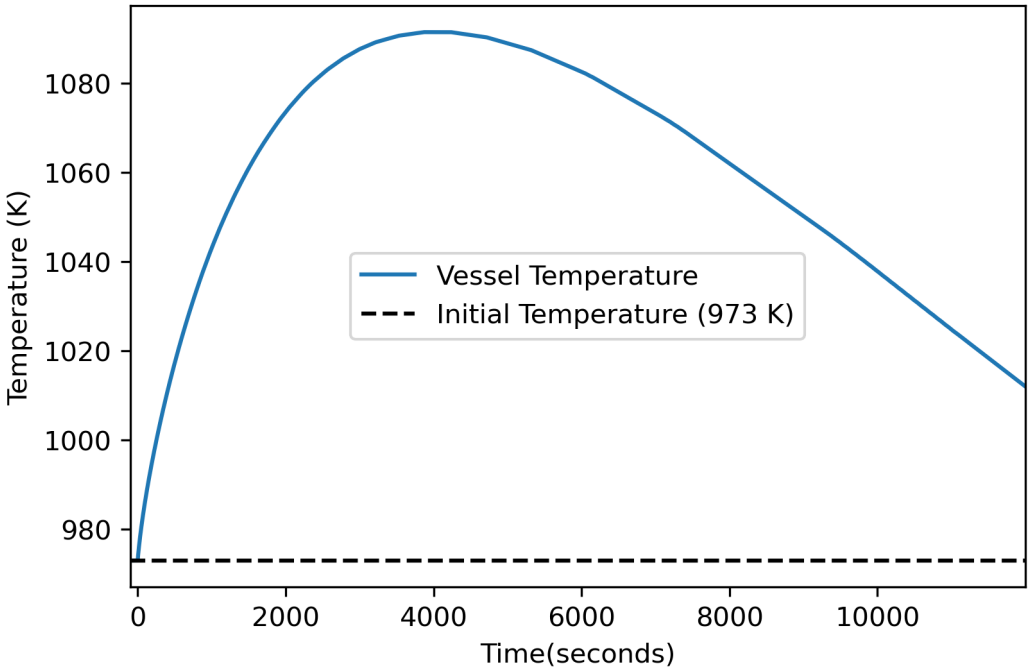

Figure 3-32. Scenario #11 Reactor Vessel Temperature

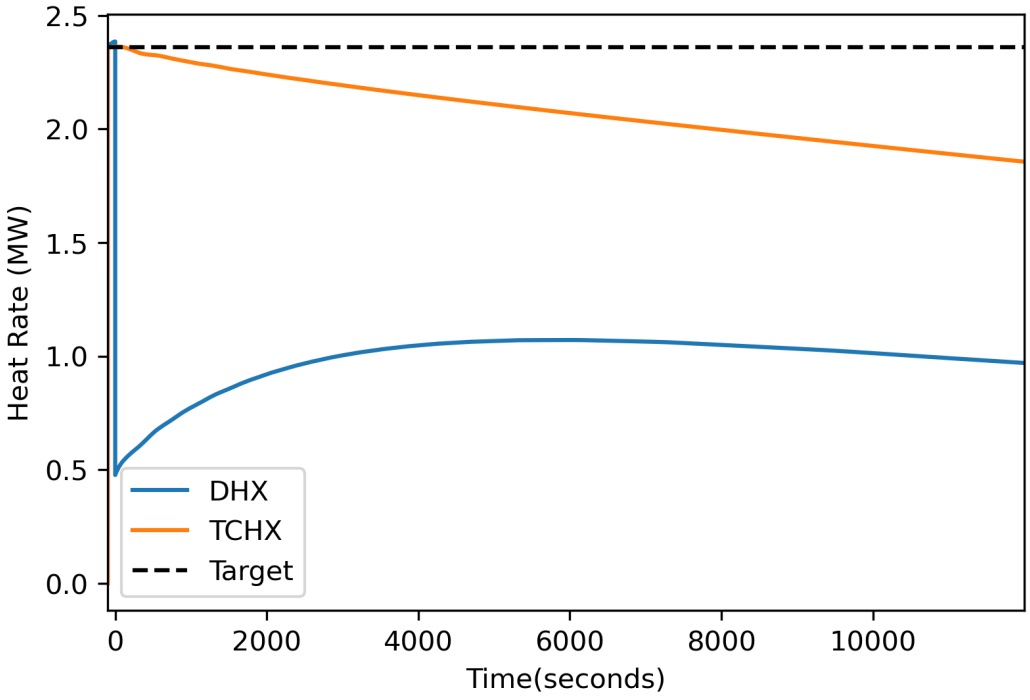

Figure 3-33. Scenario #11 Heat Exchanger heat removal rates

3.2.9. Scenario #12

Scenario #12 models the DRACS performance when all three DRACS loops are available, with the DHX operating at 10% capacity. The maximum temperature reached was 1206.5 K. After 3.5 hours, the reactor temperature was decreasing, but had not yet reached the operational temperature. The simulation was ended early due to computation time limits.

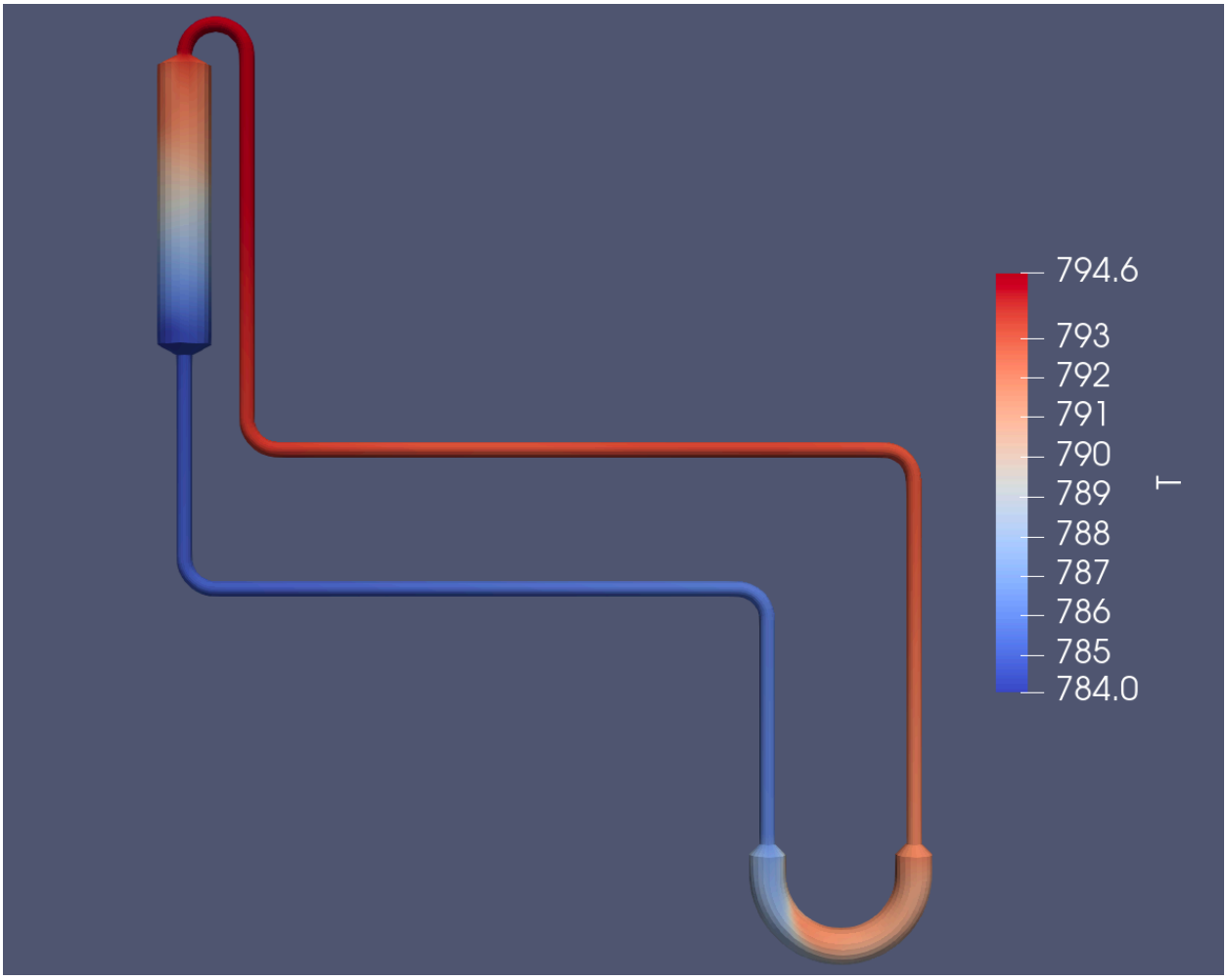

Figure 3-34. Scenario #12 Dracs loop temperature distribution one hour after the accident.

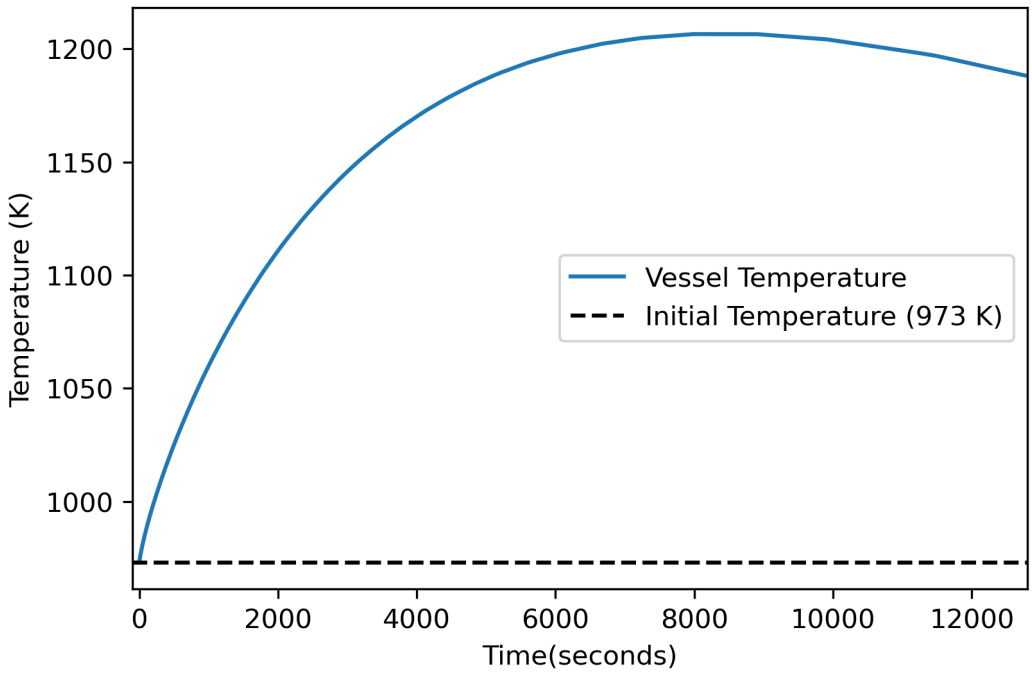

Figure 3-35. Scenario #12 Reactor Vessel Temperature

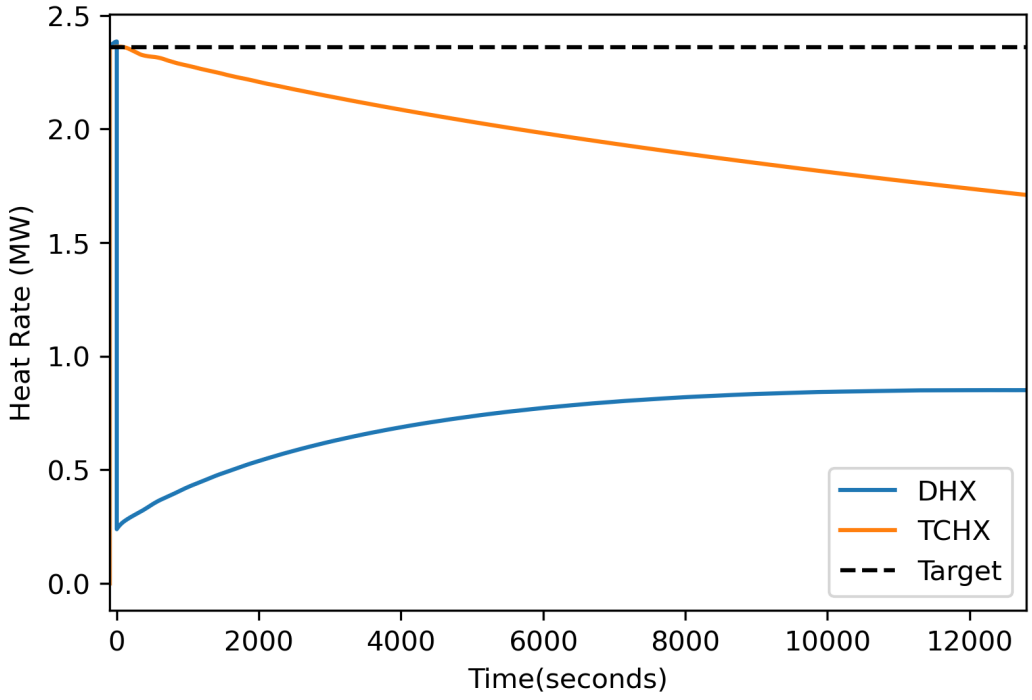

Figure 3-36. Scenario #12 Heat Exchanger heat removal rates

3.3. TCHX Degradation Scenarios

Scenarios #13-#21 investigate the effects of degraded TCHX performance. For these cases, it is assumed all three DRACS loops perform identically, and that TCHX performance degrades instantaneously at the start of the accident following 100 seconds of steady state operation.

3.3.1. Scenario #13

Scenario #13 models the DRACS performance when all three DRACS loops are available, with the TCHX operating at 90% capacity. The maximum temperature reached was 975.8 K. Reactor first returns to operational temperature 307.9 seconds after the accident begins.

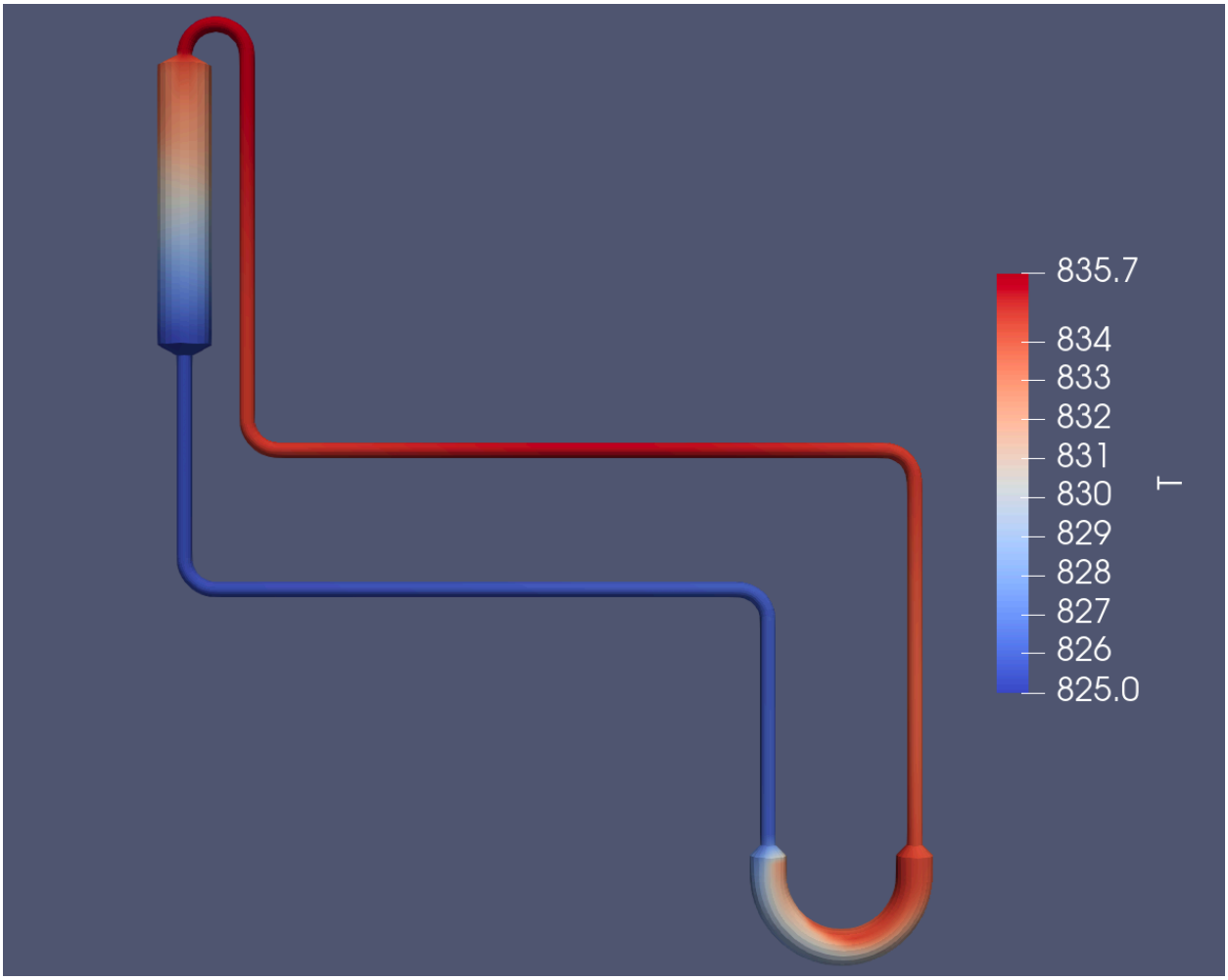

Figure 3-37. Scenario #13 Dracs loop temperature distribution one hour after the accident.

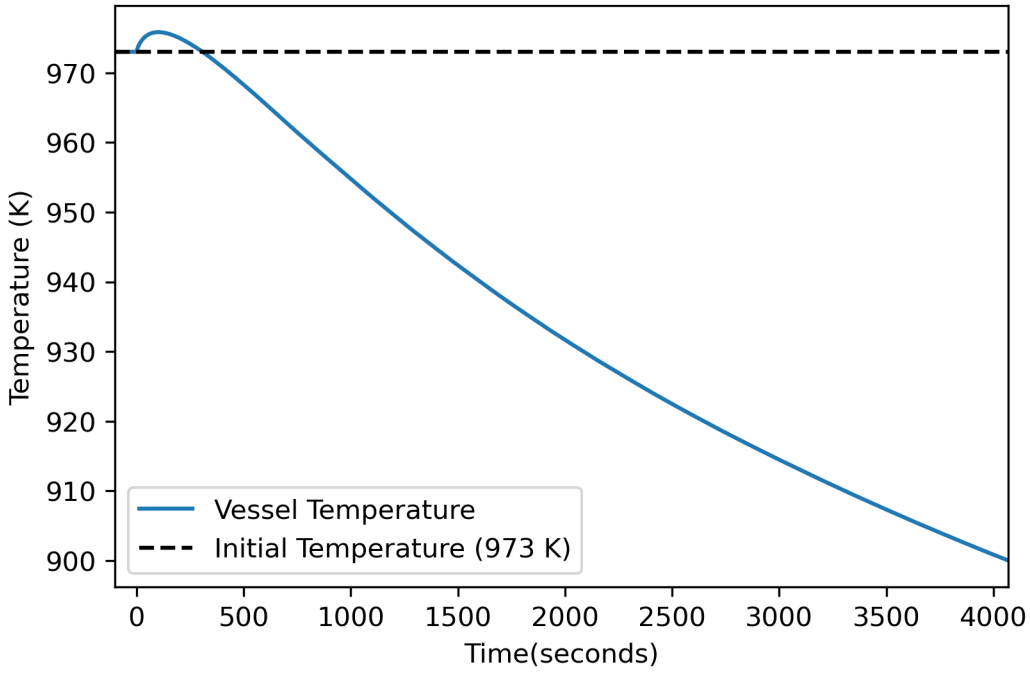

Figure 3-38. Scenario #13 Reactor Vessel Temperature

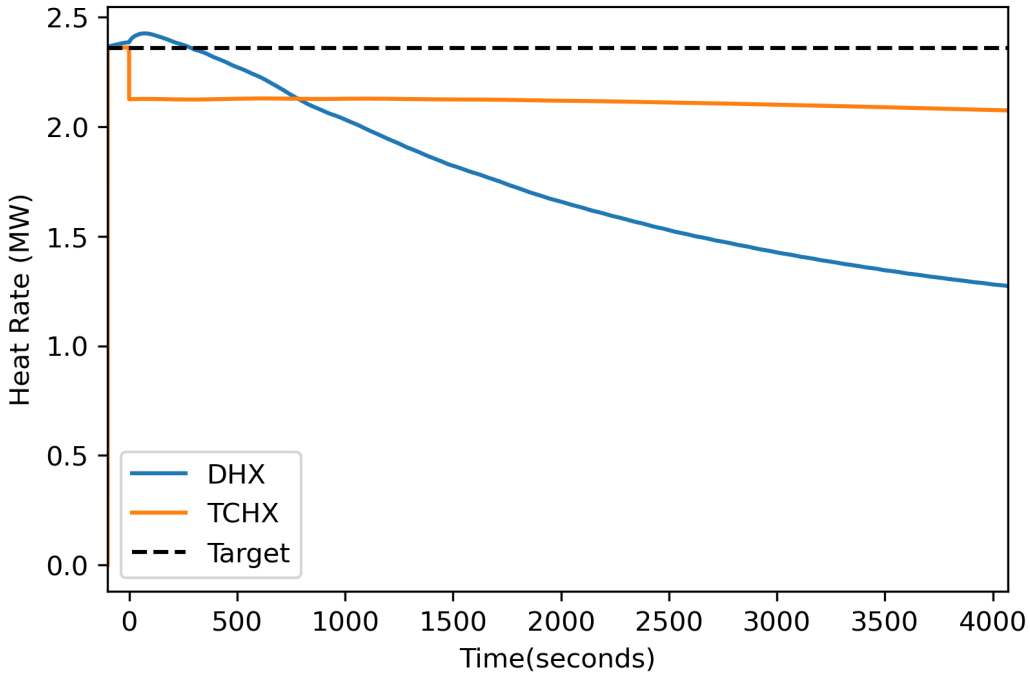

Figure 3-39. Scenario #13 Heat Exchanger heat removal rates

3.3.2. Scenario #14

Scenario #14 models the DRACS performance when all three DRACS loops are available, with the TCHX operating at 80% capacity. The maximum temperature reached was 975.8 K. Reactor first returns to operational temperature 311 seconds after the accident begins.

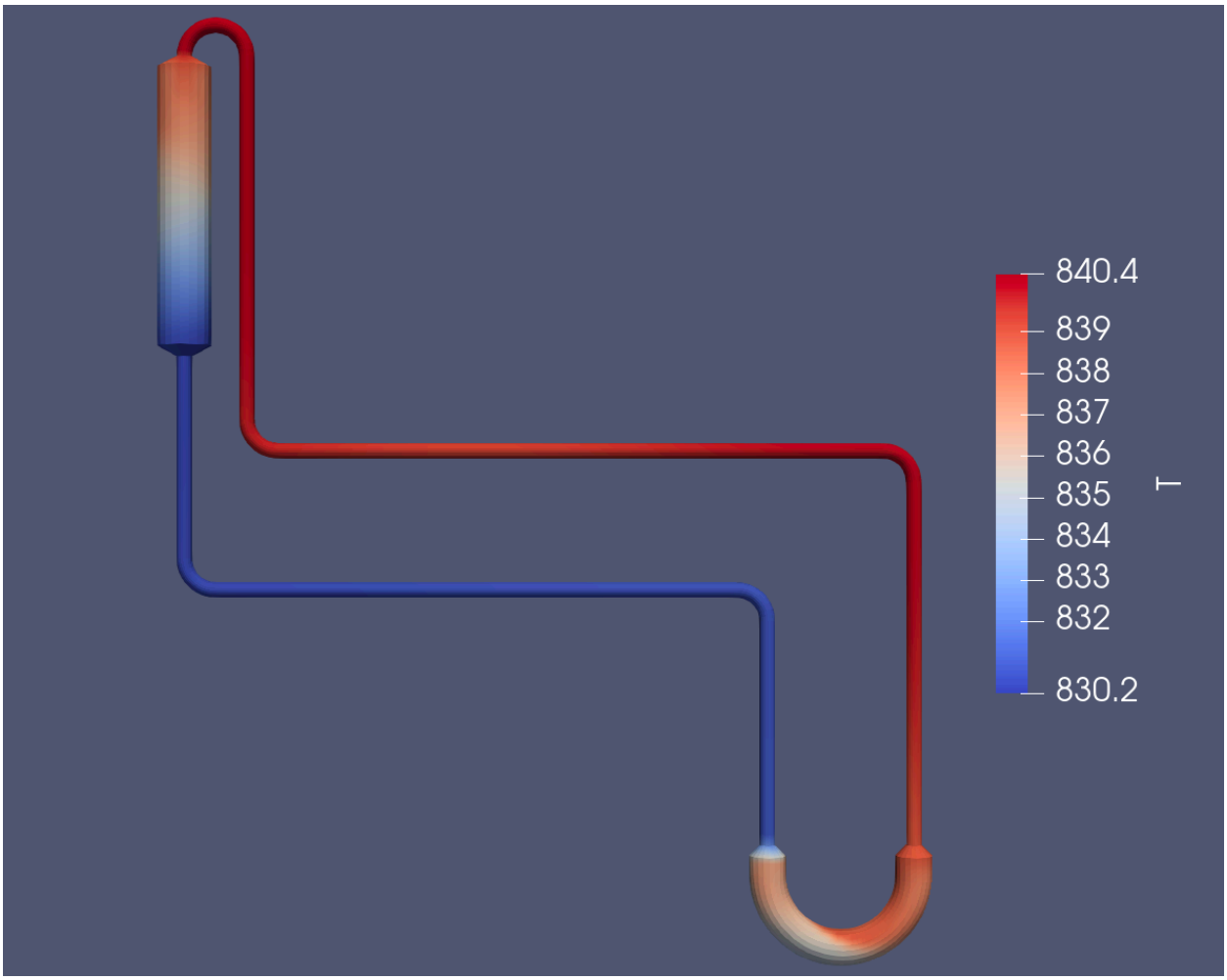

Figure 3-40. Scenario #14 Dracs loop temperature distribution one hour after the accident.

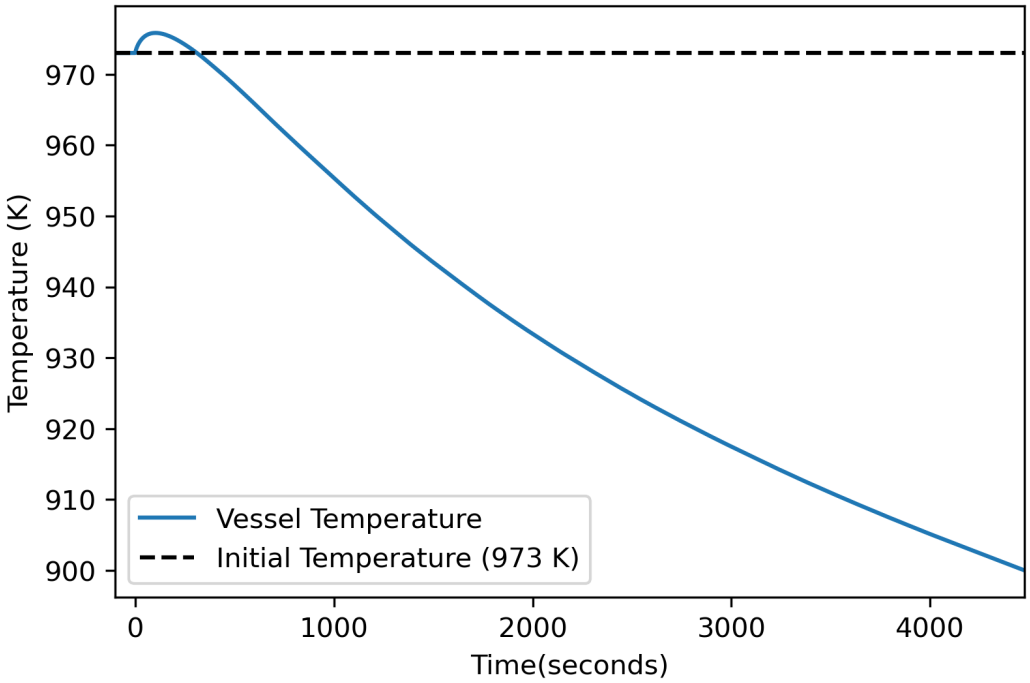

Figure 3-41. Scenario #14 Reactor Vessel Temperature

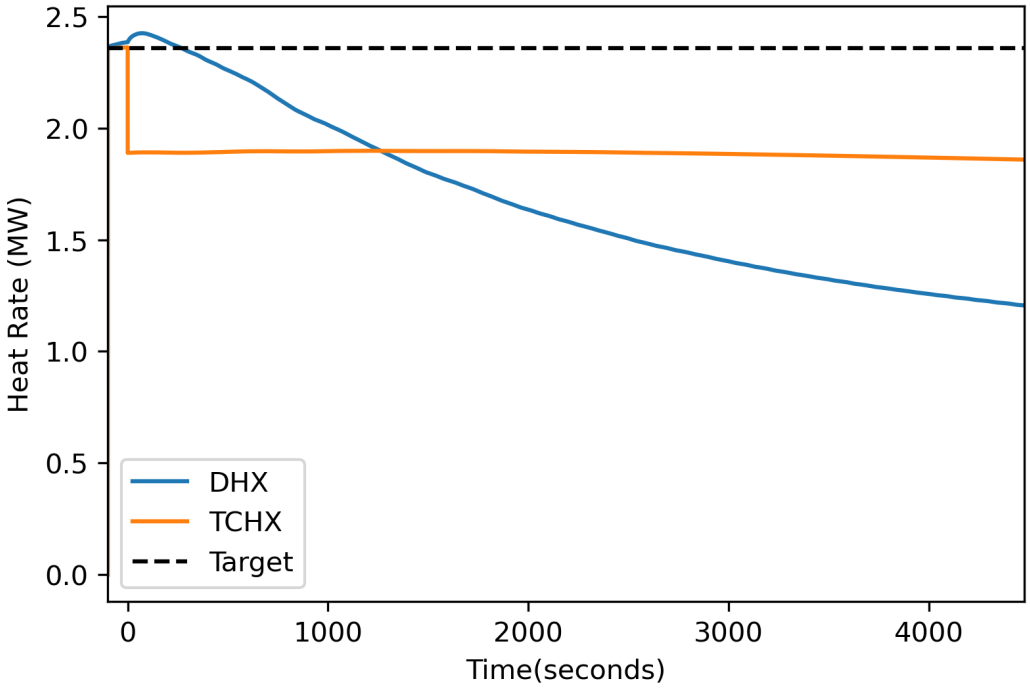

Figure 3-42. Scenario #14 Heat Exchanger heat removal rates

3.3.3. Scenario #15

Scenario #15 models the DRACS performance when all three DRACS loops are available, with the TCHX operating at 70% capacity. The maximum temperature reached was 975.8 K. Reactor first returns to operational temperature 314 seconds after the accident begins.

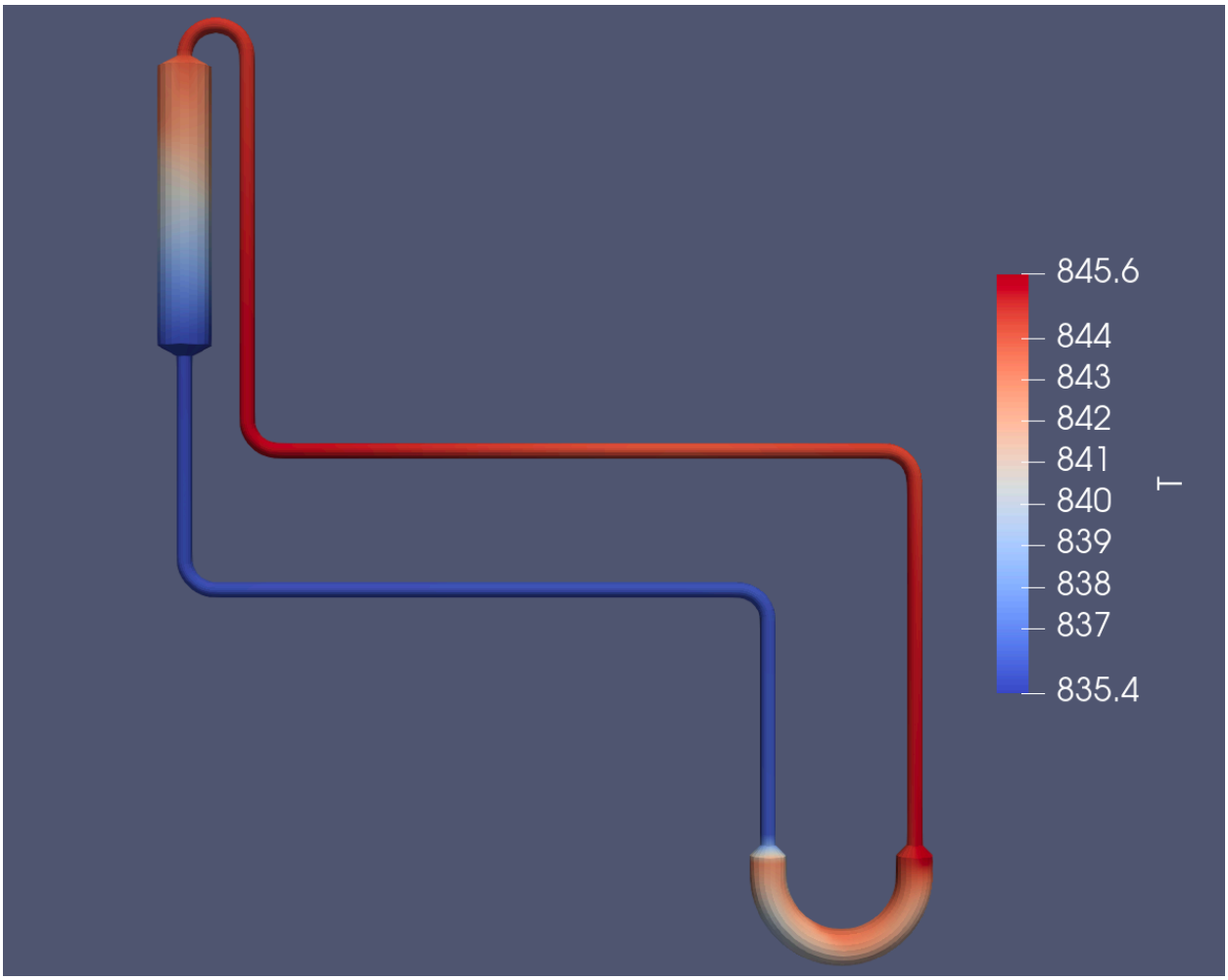

Figure 3-43. Scenario #15 Dracs loop temperature distribution one hour after the accident.

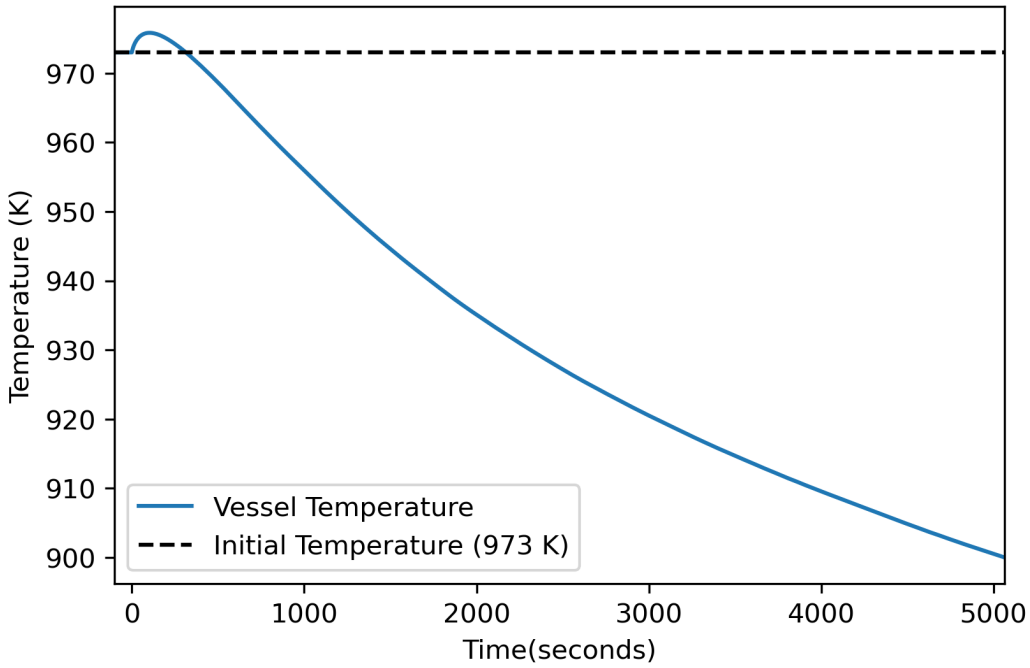

Figure 3-44. Scenario #15 Reactor Vessel Temperature

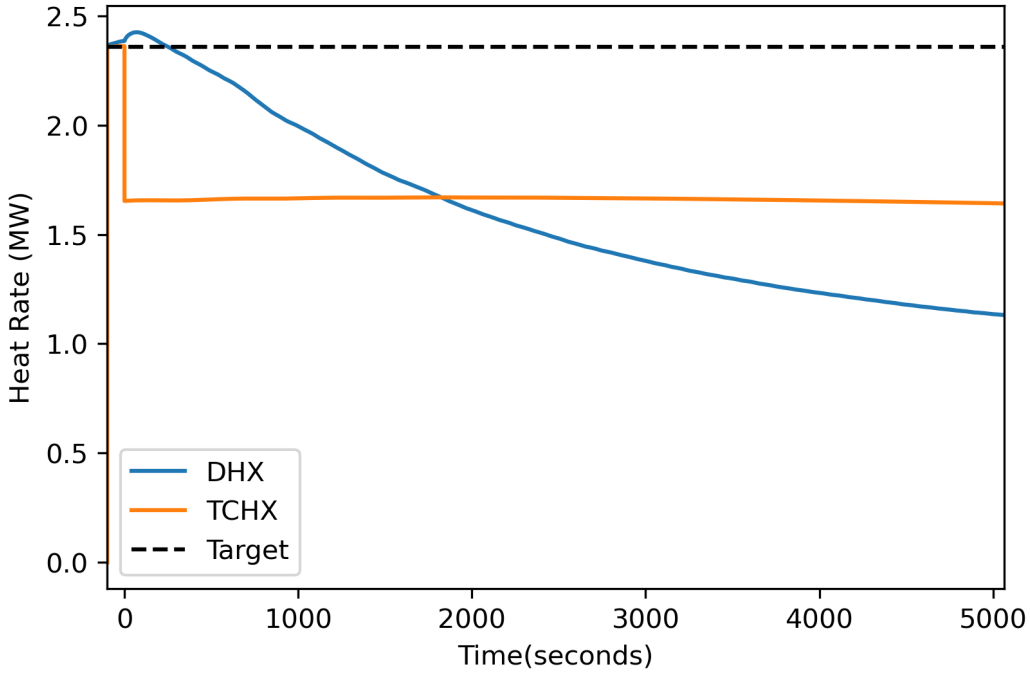

Figure 3-45. Scenario #15 Heat Exchanger heat removal rates

3.3.4. Scenario #16

Scenario #16 models the DRACS performance when all three DRACS loops are available, with the TCHX operating at 60% capacity. The maximum temperature reached was 975.8 K. Reactor first returns to operational temperature 317 seconds after the accident begins.

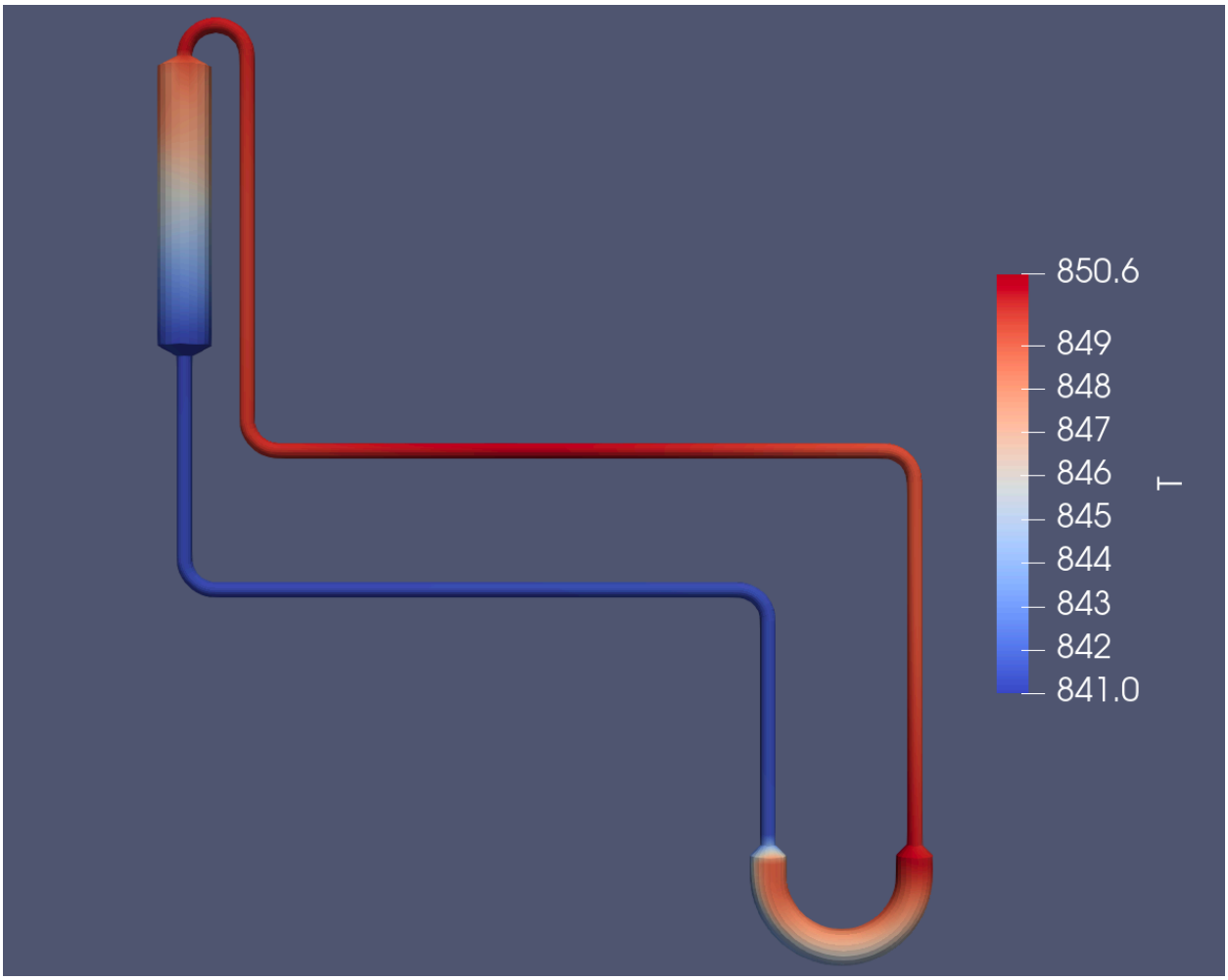

Figure 3-46. Scenario #16 Dracs loop temperature distribution one hour after the accident.

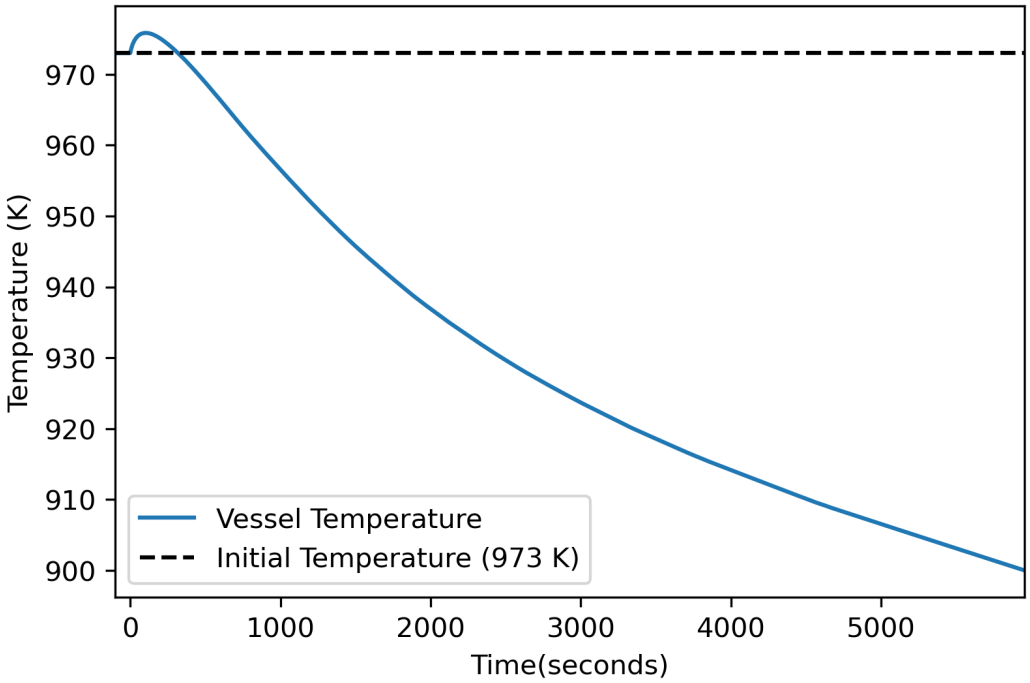

Figure 3-47. Scenario #16 Reactor Vessel Temperature

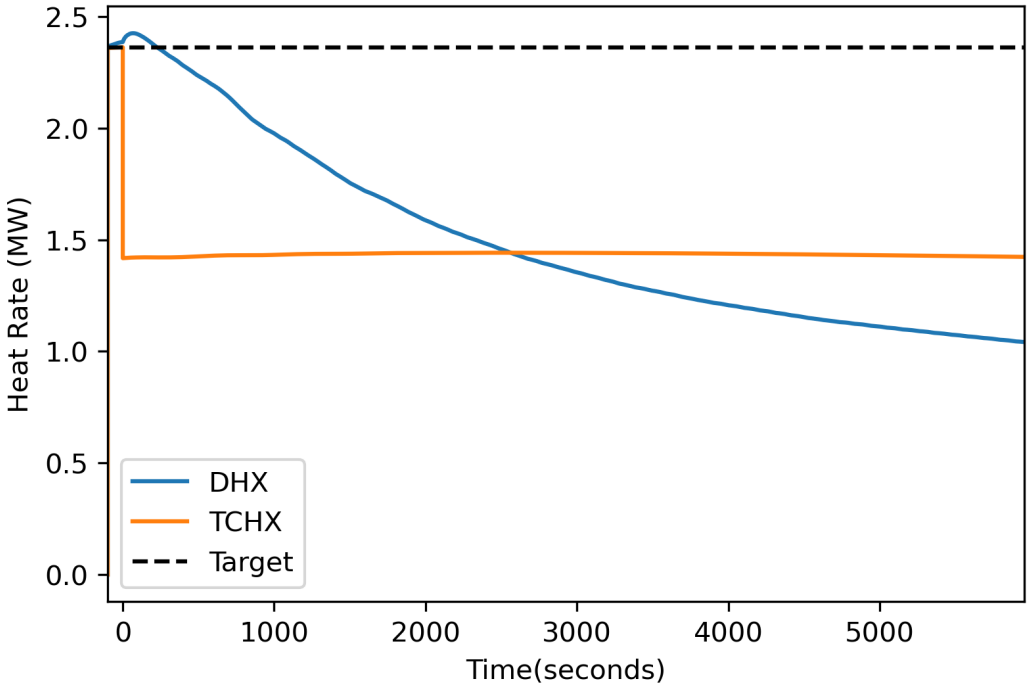

Figure 3-48. Scenario #16 Heat Exchanger heat removal rates

3.3.5. Scenario #17

Scenario #17 models the DRACS performance when all three DRACS loops are available, with the TCHX operating at 50% capacity. The maximum temperature reached was 975.8 K. Reactor first returns to operational temperature 321 seconds after the accident begins.

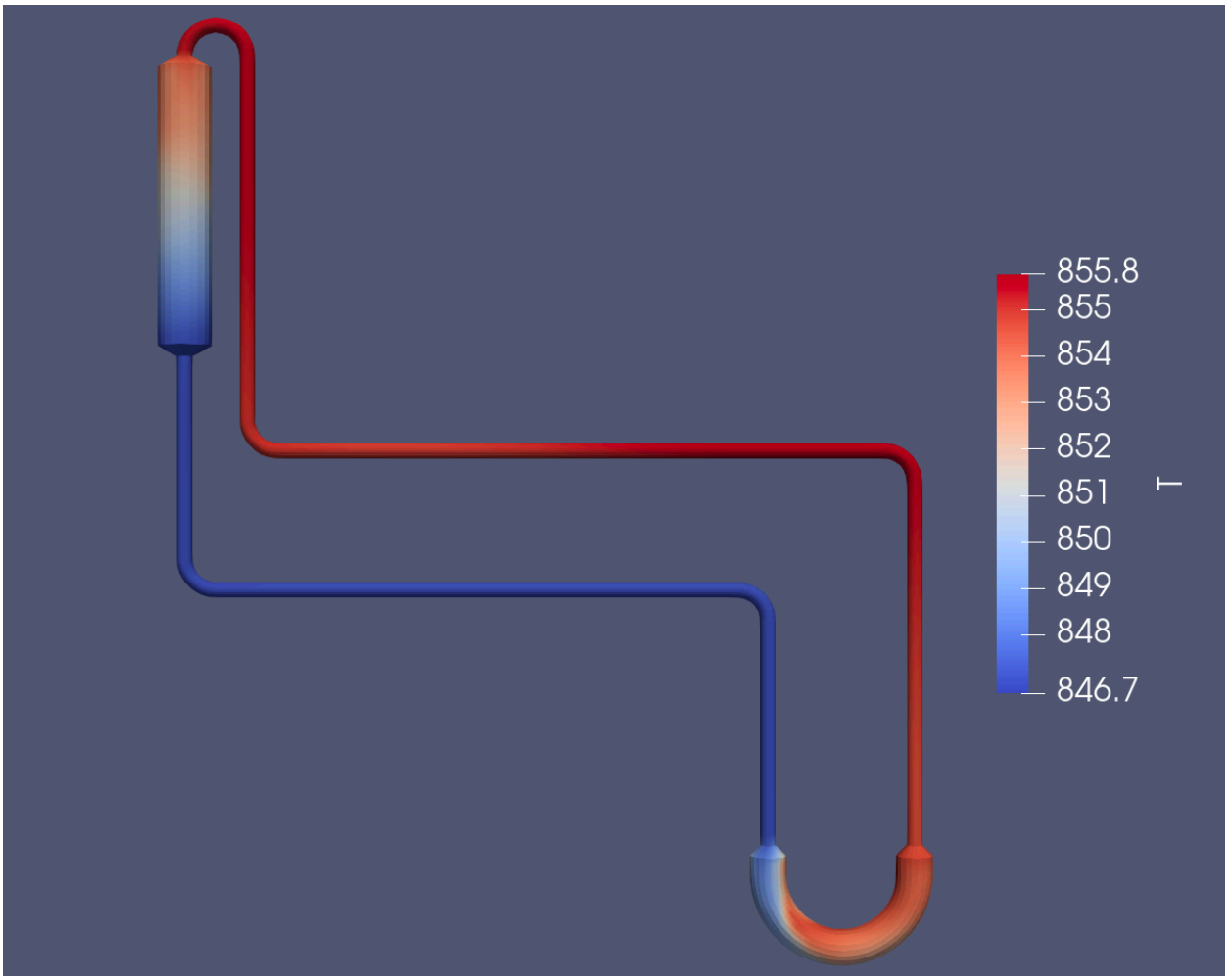

Figure 3-49. Scenario #17 Dracs loop temperature distribution one hour after the accident.

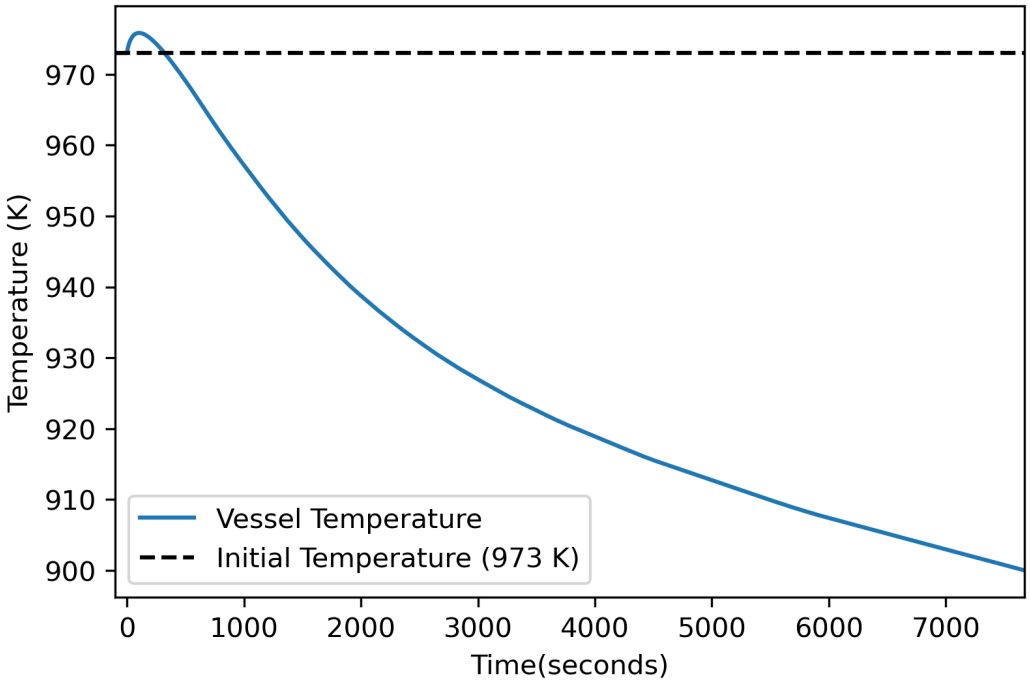

Figure 3-50. Scenario #17 Reactor Vessel Temperature

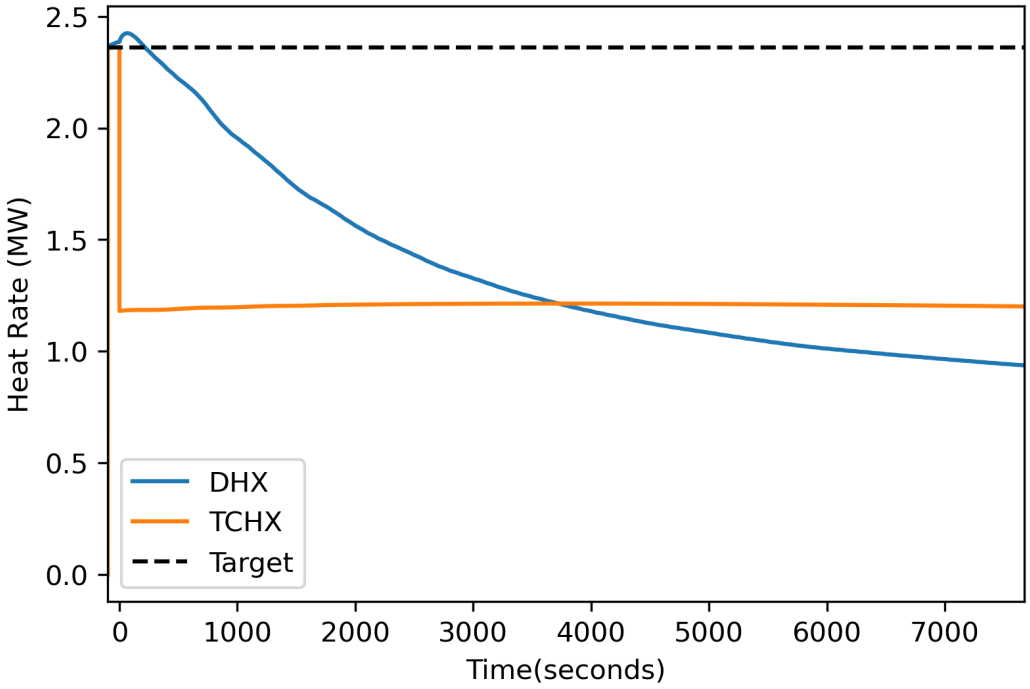

Figure 3-51. Scenario #17 Heat Exchanger heat removal rates

3.3.6. Scenario #18

Scenario #18 models the DRACS performance when all three DRACS loops are available, with the TCHX operating at 40% capacity. The maximum temperature reached was 975.8 K. Reactor first returns to operational temperature 324 seconds after the accident begins.

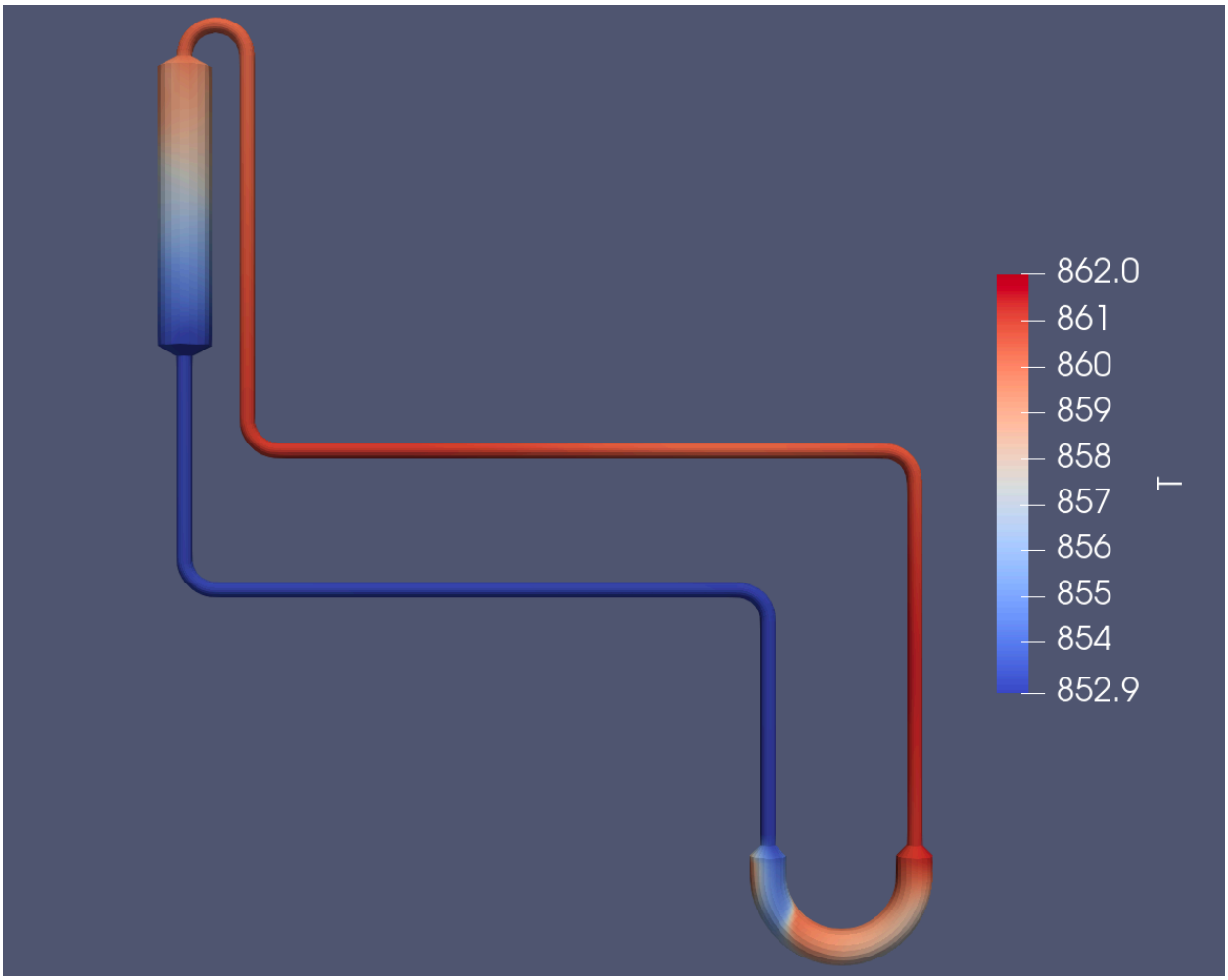

Figure 3-52. Scenario #18 Dracs loop temperature distribution one hour after the accident.

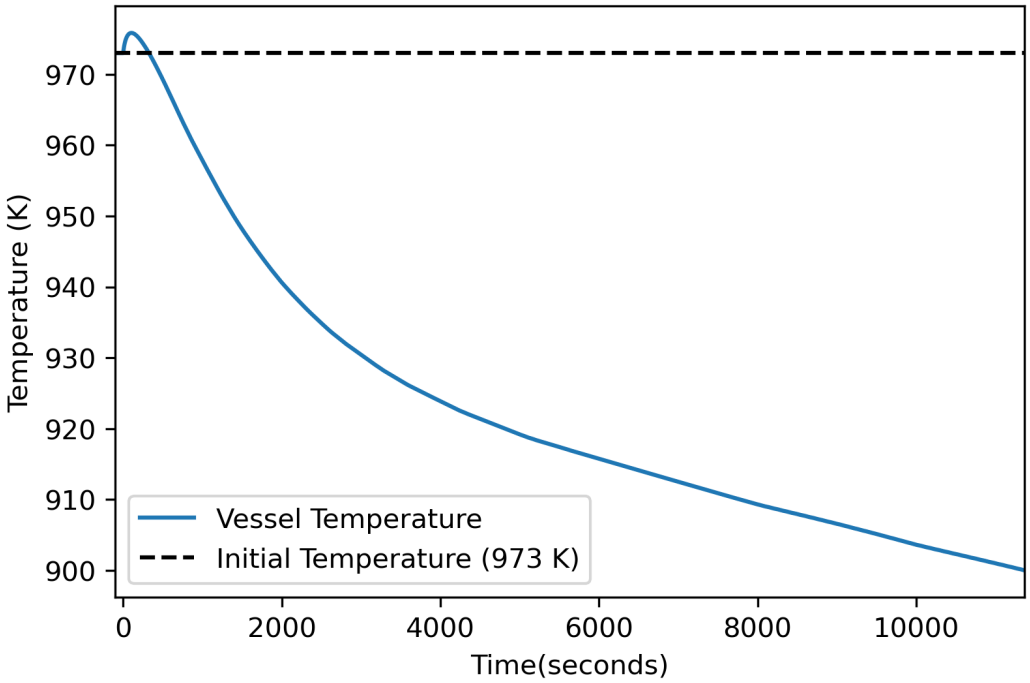

Figure 3-53. Scenario #18 Reactor Vessel Temperature

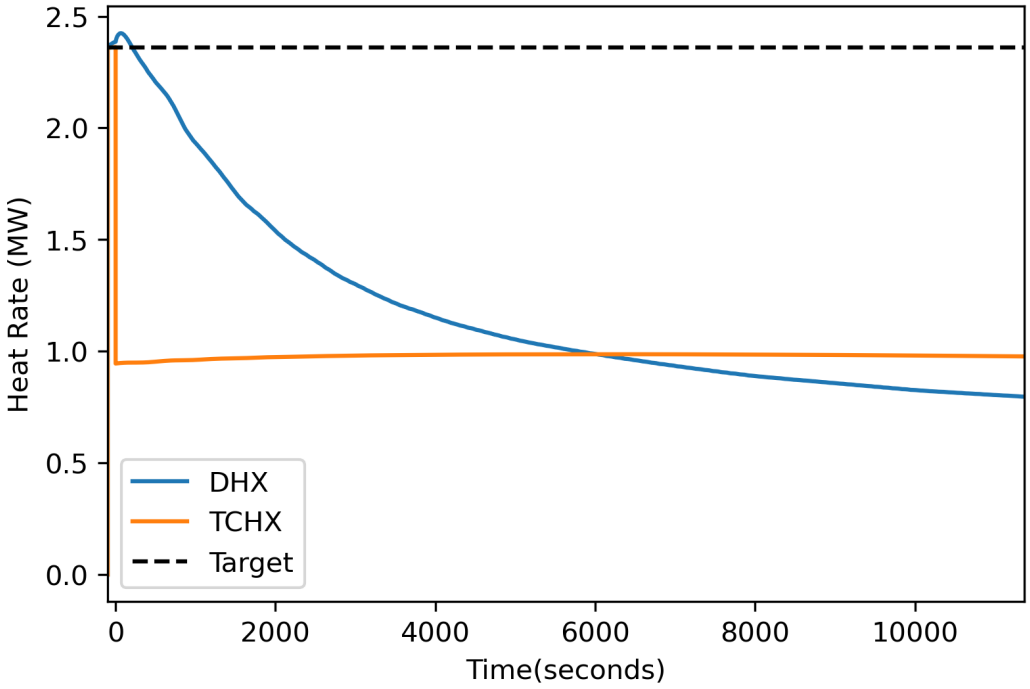

Figure 3-54. Scenario #18 Heat Exchanger heat removal rates

3.3.7. Scenario #19

Scenario #19 models the DRACS performance when all three DRACS loops are available, with the TCHX operating at 30% capacity. The maximum temperature reached was 975.8 K. Reactor first returns to operational temperature 328 seconds after the accident begins.

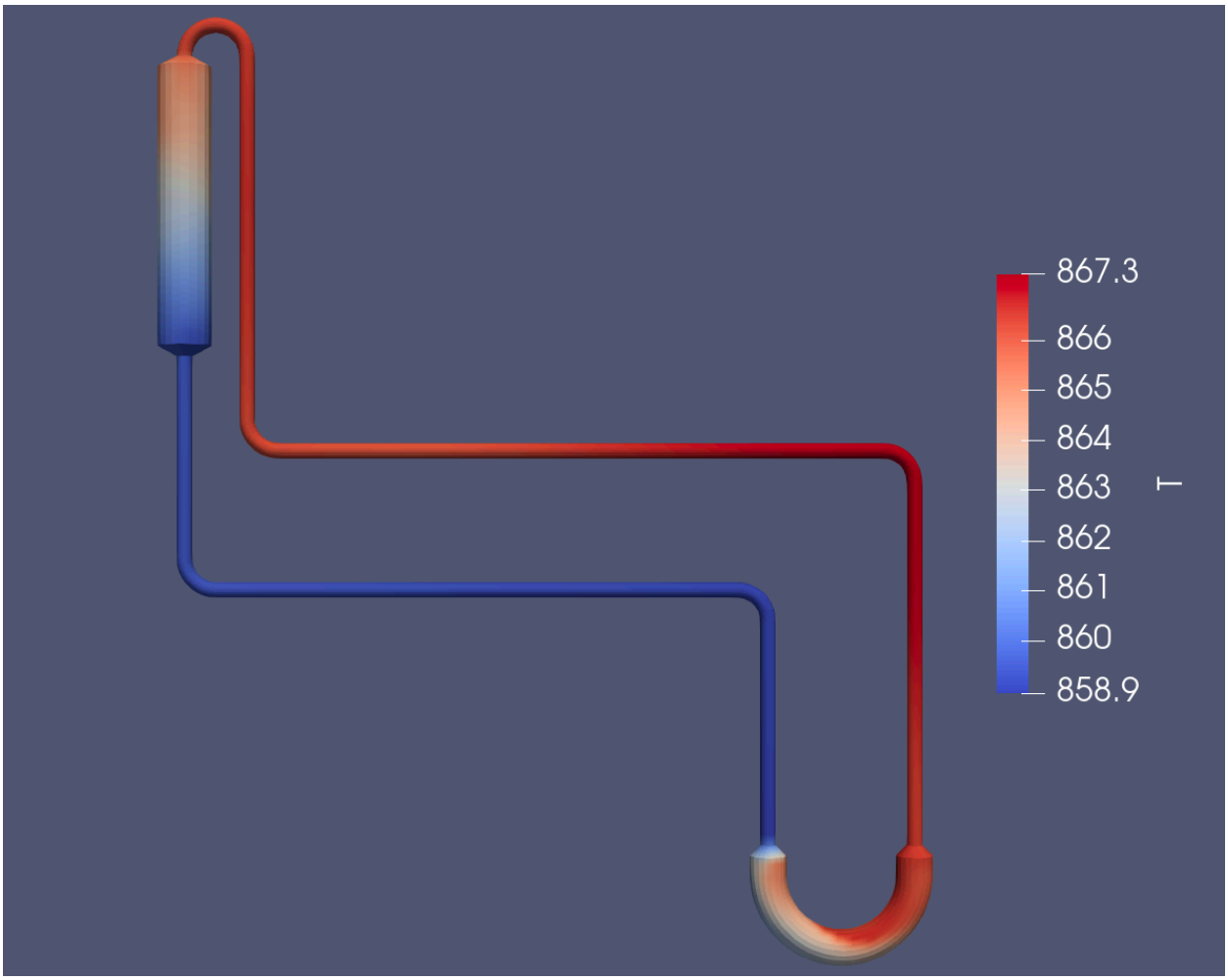

Figure 3-55. Scenario #19 Dracs loop temperature distribution one hour after the accident.

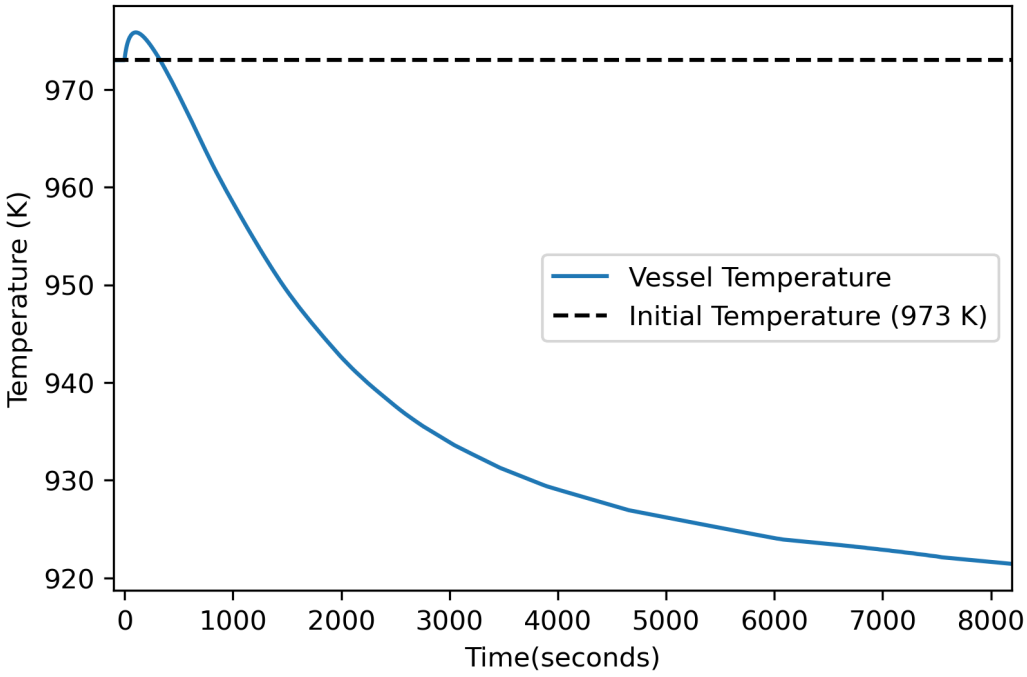

Figure 3-56. Scenario #19 Reactor Vessel Temperature

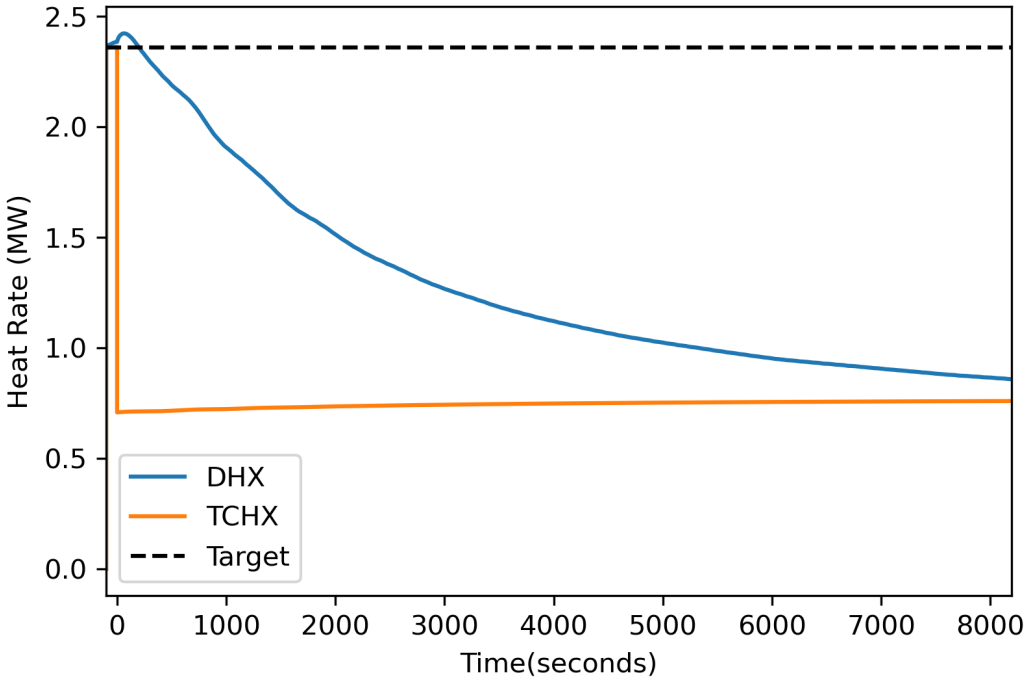

Figure 3-57. Scenario #19 Heat Exchanger heat removal rates

3.3.8. Scenario #20

Scenario #20 models the DRACS performance when all three DRACS loops are available, with the TCHX operating at 20% capacity. The maximum temperature reached was 975.8 K. Reactor first returns to operational temperature 332 seconds after the accident begins. An important note, at this level of degradation, the reactor vessel temperature begins to increase again after a few hours of cooling. This is due to the DRACS loop heating up to the point that it cannot remove enough heat to match the decay heat generation rate.

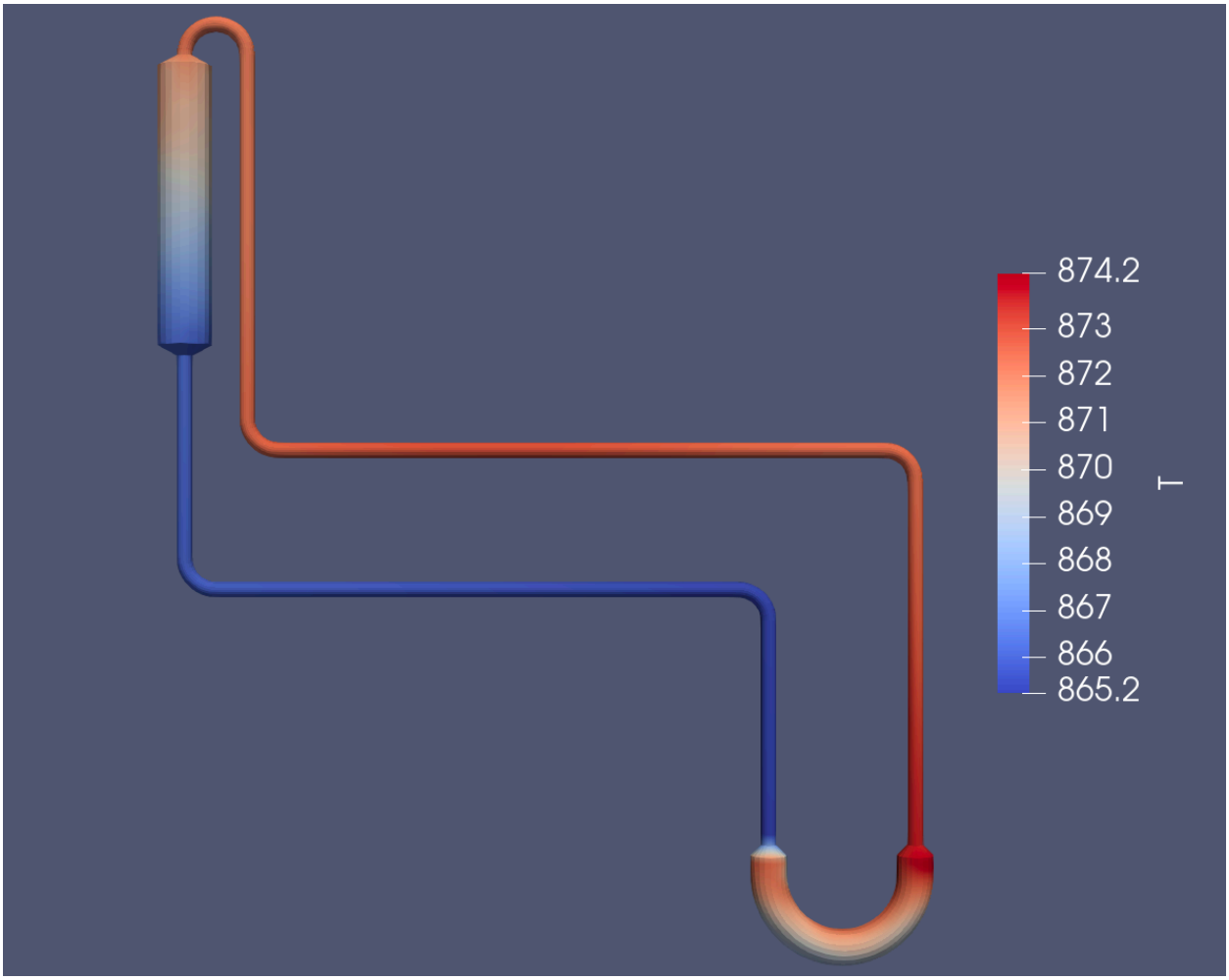

Figure 3-58. Scenario #20 Dracs loop temperature distribution one hour after the accident.

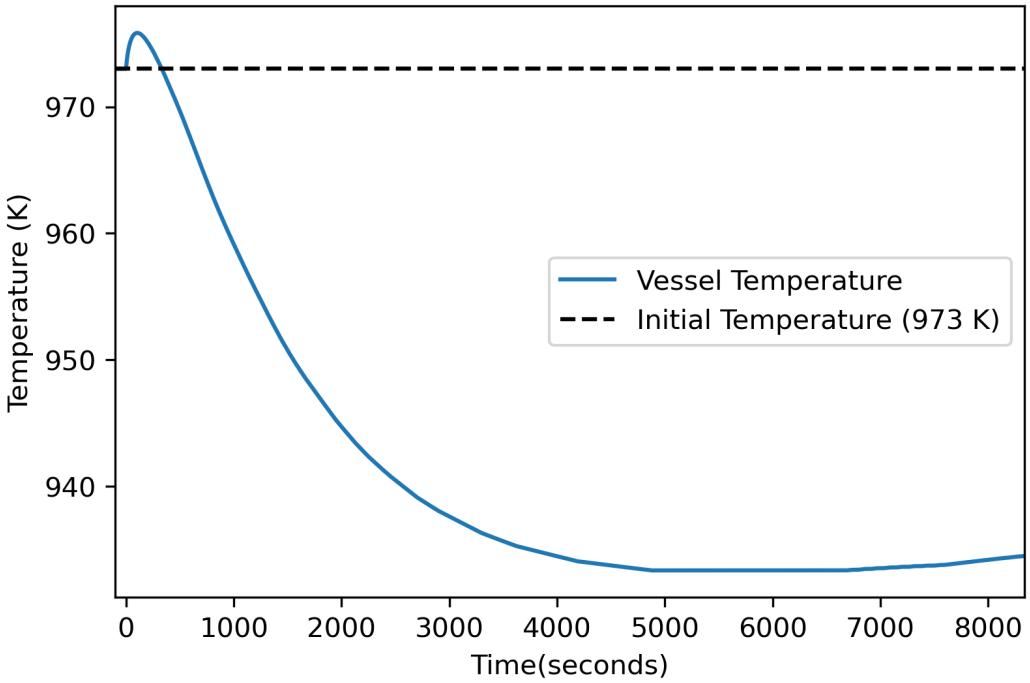

Figure 3-59. Scenario #20 Reactor Vessel Temperature

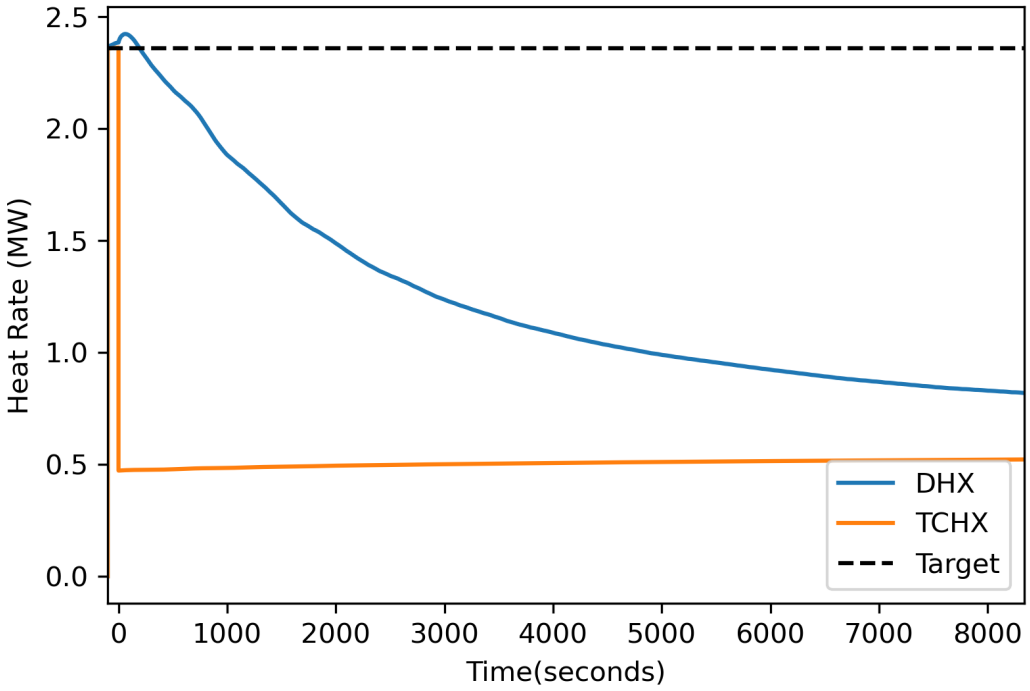

Figure 3-60. Scenario #20 Heat Exchanger heat removal rates

3.3.9. Scenario #21

Scenario #21 models the DRACS performance when all three DRACS loops are available, with the TCHX operating at 10% capacity. The maximum temperature reached was 975.8 K. Reactor first returns to operational temperature 337 seconds after the accident begins. As seen in the previous case, at such degraded levels of TCHX performance, the reactor vessel will begin to warm up again after a few hours of cooling. This is due to heating of the DRACS loop since the heat has nowhere to go. Further investigation is warranted to evaluate longer-term operation of a DRACS with degraded TCHX.

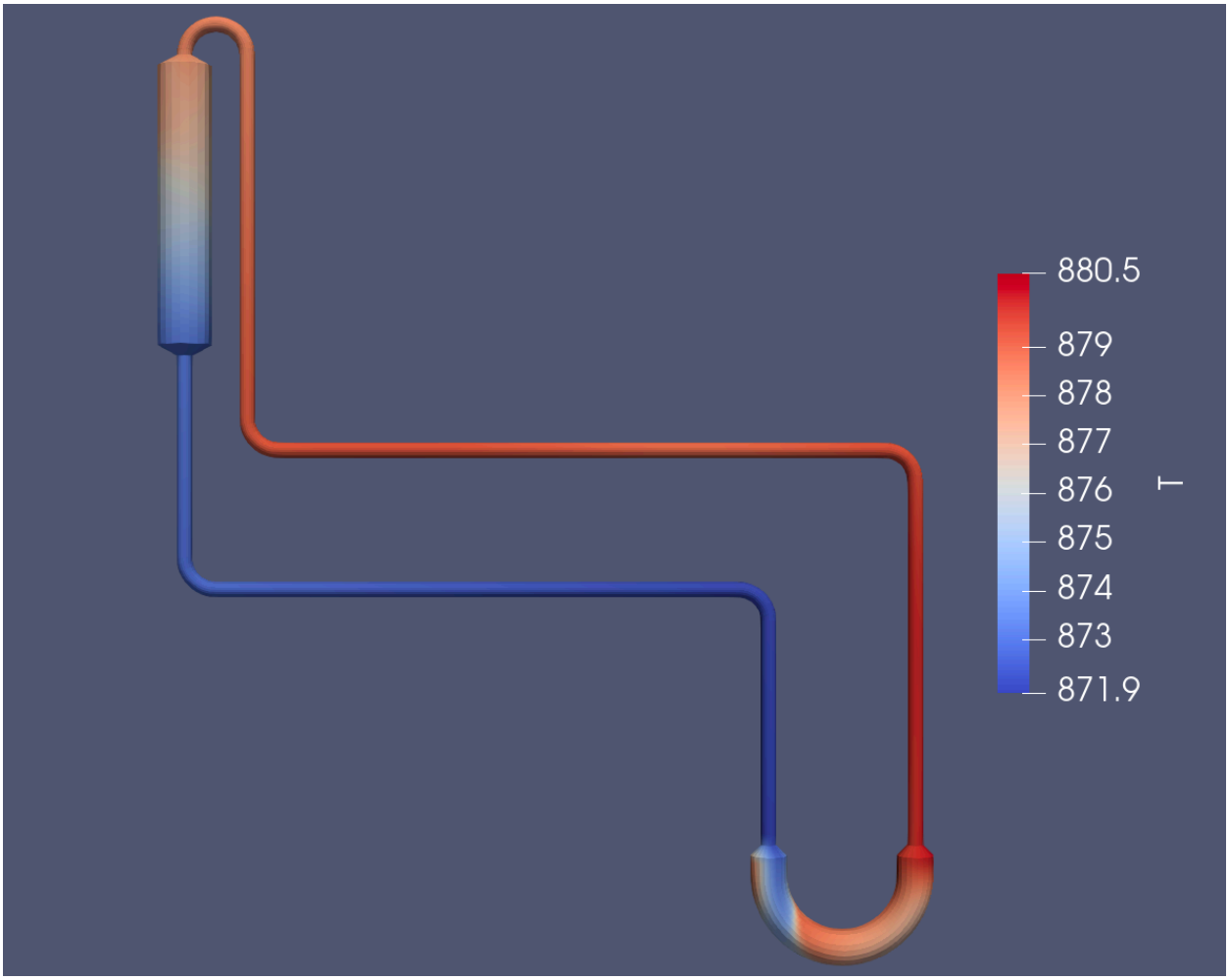

Figure 3-61. Scenario #21 Dracs loop temperature distribution one hour after the accident.

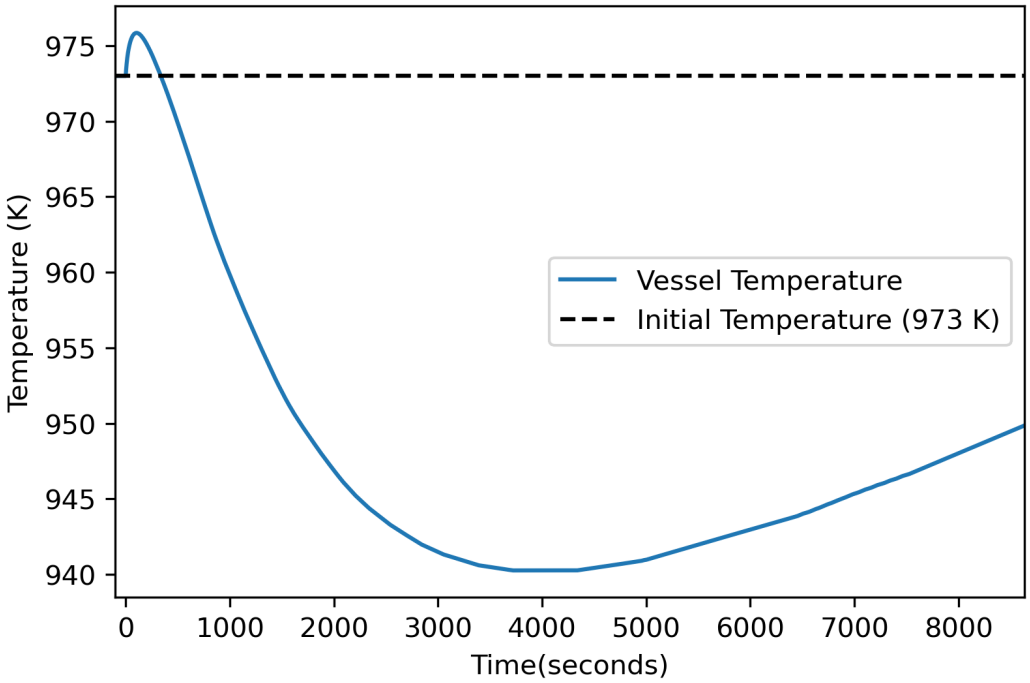

Figure 3-62. Scenario #21 Reactor Vessel Temperature

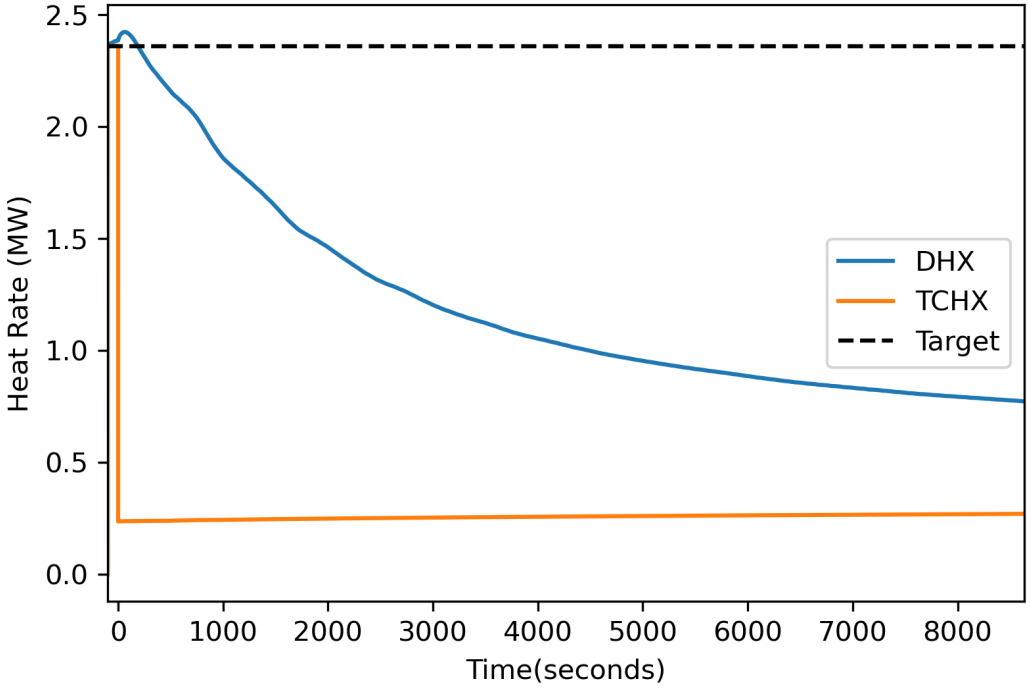

Figure 3-63. Scenario #21 Heat Exchanger heat removal rates

3.4. Summary of Results

Table 3-1. Summary of degradation study results.

Scenario #	Maximum Reactor Temperature (K)	Time until reactor falls below operation temperature (s)	DRACS max temperature after one hour (K)
1	975.8	305	831
2	986.8	1980	844
3	1046.1	Not reached during test	864
4	977.4	510	830
5	980.0	866	830
6	984.3	1446	827
7	991.0	2309	825
8	1001.6	3586	822
9	1018.0	5524	819
10	1044.2	8814	814
11	1091.4	Not reached during test	806
12	1206.5	Not reached during test	795
13	975.8	308	836
14	975.8	311	840
15	975.8	314	846
16	975.8	317	851
17	975.8	321	856
18	975.8	324	862
19	975.8	328	867
20	975.8	332	874
21	975.8	337	881

4. CONCLUSION

The direct reactor auxiliary cooling system is a very robust, passive safety system that is designed to remove up to 2.36 MW of heat from the reactor during accident conditions. This report details a variety of DRACS degradation conditions and their effect on the safety of the reactor. This preliminary investigation shows that only two of the three DRACS loops are necessary to quickly suppress the decay heat produced by a newly shut down reactor. Even with a single DRACS loop operational, the maximum salt temperature observed was far below the safety specification of the plant (1173 K). When investigating the degraded performance of each DRACS loop, the short-term maximum salt temperature observed was strongly dependent on the DHX performance but was unaffected by the TCHX performance. However, even a heavily degraded DHX heat transfer performance was sufficient to halt the rising salt temperature due to decay heat. Further investigation should be done to characterize the effects of TCHX performance degradation at longer time scales. High levels of TCHX degradation were shown to lead to a reactor salt temperature minimum after a few hours of operation followed by a steady increase in temperature. With reduced ability to exhaust heat to the environment, it is possible the DRACS would be unable to maintain cooling during a long loss of active cooling event. This investigation would benefit from additional tests over long time scales, as well as an evaluation of the combined effects of degradation if both

REFERENCES

[1] Department of Nuclear Engineering, University of California, Berkeley, "Technical Description of the “Mark 1” Pebble-Bed Fluoride-Salt-Cooled High-Temperature Reactor (PB-FHR) Power Plant," 30 September 2014. [Online]. Available: https://web.mit.edu/nse/pdf/researchstaff/forsberg/FHR%20Point%20Design%2014-002%20UCB.pdf. [Accessed 27 September 2021].

[2] M. S. Sohal, M. A. Ebner, P. Sabharwall and P. Sharpe, "Engineering Database of Liquid Salt Thermophysical and Thermochemical Properties," June 2013. [Online]. Available: https://inldigitallibrary.inl.gov/sites/STI/STI/5698704.pdf.

[3] OpenCFD Ltd., "OpenFOAM User Guide: v2012," [Online]. Available: https://www.openfoam.com/documentation/guides/latest/doc/guide-bcs-wall-turbulence-omegaWallFunction.html. [Accessed 27 September 2021].

5. APPENDIX

A.1. Tabulated Decay Heat Rate as a Function of Time

Table A-1. Table of decay heat rate as a function of time since reactor scram.

Time since Reactor Scram (s)	Decay Heat Rate (W)
0.0	14695160.0
1.0	13660590.0
1.321762	13430340.0
1.747055	13165480.0
2.309192	12866390.0
3.052203	12534680.0
4.034286	12173150.0
5.332367	11785490.0
7.048121	11376270.0
9.315941	10950950.0
12.31346	10515810.0
16.27547	10077240.0
21.51229	9640521.0
28.43414	9207844.0
37.58317	8777661.0
49.67602	8347339.0
65.65989	7917752.0
86.78676	7495247.0
114.7115	7089419.0
151.6213	6708813.0

Time since Reactor Scram (s)	Decay Heat Rate (W)
200.4073	6357635.0
264.8908	6034599.0
350.1226	5733366.0
462.7789	5444705.0
611.6837	5159279.0
808.5003	4870379.0
1068.645	4574686.0
1412.495	4271920.0
1866.982	3964821.0
2467.707	3659017.0
3261.722	3361219.0
4311.221	3077196.0
5698.409	2810341.0
7531.941	2562356.0
9955.436	2334841.0
13158.72	2130275.0
17392.7	1950380.0
22989.01	1792782.0
30386.01	1650724.0
40163.08	1517311.0
53086.04	1389825.0
70167.12	1268852.0
92744.25	1155348.0
122585.9	1049072.0

Time since Reactor Scram (s)	Decay Heat Rate (W)
162029.3	949073.7
214164.3	853924.8
283074.2	763812.6
374156.9	677486.7
494546.4	594940.9
653672.8	517477.6
864000.0	408533.5

A.2. Salt Thermophysical Properties

Table A-2. Thermophysical properties of FLiBe used in calculations.

Property	Value	Source
T_{ref} (K)	975	MELCOR FliBe properties
Density (kg/m^3)	1918.5	MELCOR FliBe properties
Thermal Expansion Coefficient (K^{-1})	2.28×10^{-4}	MELCOR FliBe properties
Heat Capacity (kJ/kg-K)	2414.17	INL Engineering Database [2]
Dynamic viscosity (Pa-s)	0.0210	INL Engineering Database [2]
Prandtl Number	25.327	INL Engineering Database [2]